

Bechtel Bettis, Inc.
Bettis Atomic Power Laboratory
West Mifflin, Pennsylvania

**Materials Technology
Advanced Materials System Integration**

TITLE: Alternator Electrical Feedthrough Insulator Materials for Project
Prometheus [B-MT(AMSI)-44]

AUTHOR: Jason K. Clobes and Andrew M. Ruminski

CONTRIBUTORS: John P. D'Antonio and Aaron M. Datesman

DATE: JAN 4 2006

SIGNIFICANCE TO THE NR PROGRAM:

The notional Naval Reactors Prime Contractor Team (NRPCT) propulsion plant concept for the Jupiter Icy Moons Orbiter (JIMO) space mission was based on a gas-cooled Brayton system intended to operate at high temperature for over fifteen years without maintenance. A critical issue that was identified for the Brayton application is the potential leakage of system coolant gases through the alternator electrical feedthroughs. Literature research and vendor consultation were performed to determine applicable electrical insulator/conductor designs and material combinations for the feedthroughs. This report explores the insulator materials options available and provides recommendations for future actions that could have been implemented had the space program continued in Naval Reactors (NR). Based on the initial evaluation of vendor capabilities, hermetic electrical feedthrough technology should currently be available to meet the requirements of a Prometheus mission. A limited development effort may be required to refine the feedthrough materials and design. Exhaustive testing would be essential to verify component integrity throughout the fifteen year maintenance-free lifetime.

EXECUTIVE SUMMARY:

The potential leakage of helium and xenon coolant gases through the electrical feedthroughs for the Brayton cycle space nuclear power plant was identified as a critical issue to the success of the Prometheus mission. Literature studies suggested that ceramic/metal, glass-ceramic/metal, and glass/metal seals could all potentially be used in these feedthroughs. Ceramics, especially alumina, are widely applied in the electrical feedthrough industry, and provide good mechanical, thermal, and electrical properties. However, glasses provide ease of processing and can be tailored to more precise thermal expansion characteristics than ceramics, which is important in minimizing thermal stresses. The characteristics of glass-ceramics are in between that of ceramics and glasses, and may provide coefficient of thermal expansion (CTE) matching along with enhanced properties.

Studies of the available vendors suggested that a number of commercial vendors produce hermetic ceramic and glass insulated electrical feedthroughs that are potentially applicable to this application. Had the space program continued, it would have been recommended to procure and test several commercial power feedthroughs of varying materials combinations. Results of the initial testing would have then dictated subsequent procedures.

TABLE OF CONTENTS

| | |
|---|-----|
| Significance to the NR Program..... | 1 |
| Executive Summary..... | 1 |
| Table of Contents | 2 |
| List of Figures | 3 |
| List of Tables | 3 |
| 1.0 Introduction..... | 4 |
| 2.0 Background..... | 4 |
| 2.1 Alternator Description..... | 4 |
| 2.2 Electrical Feedthrough Gas Leakage Concerns..... | 6 |
| 3.0 Glass/Metal and Glass-Ceramic/Metal Seals | 10 |
| 3.1 Mechanical Integrity of Glass/Metal Seals | 11 |
| 3.2 Chemical Integrity of Glass/Metal Seals | 14 |
| 3.3 Electrical Integrity of Glass/Metal Seals..... | 18 |
| 4.0 Ceramic/Metal Seals | 19 |
| 4.1 Mechanical Integrity of Ceramic/Metal Seals | 20 |
| 4.2 Chemical Integrity of Ceramic/Metal Seals | 22 |
| 4.3 Electrical Integrity of Ceramic/Metal Seals..... | 22 |
| 5.0 Polymer/Metal Seals | 22 |
| 6.0 Proposed Testing..... | 23 |
| 6.1 Initial Helium Leak Testing | 23 |
| 6.2 Initial Mechanical and Electrical Property Testing..... | 25 |
| 7.0 Potential Vendors..... | 26 |
| 8.0 Summary and Conclusions | 29 |
| References | 30 |
| Appendix A: Concepts in the Joining of Metals to Rigid Materials..... | A1 |
| A.1 Introduction..... | A3 |
| A.2 Seal Design | A4 |
| A.3 Surface Wetting | A7 |
| A.4 Bonding and Interfacial Reactions..... | A7 |
| A.5 Metal Brazing | A8 |
| A.6 Indirect Brazing and Metallizing of a Ceramic Surface | A9 |
| A.7 Solid State or Diffusion Bonding..... | A9 |
| A.8 Direct Bonding or Fusion Welding..... | A10 |

LIST OF FIGURES

| | |
|--|----|
| Figure 1: Space Brayton turboalternator conceptual design | 5 |
| Figure 2: Hamilton Sundstrand turboalternator external design depicting feedthrough lead positions | 5 |
| Figure 3: Simplified schematic of electrical feedthrough assembly | 7 |
| Figure 4: Schematic of components and assembly of a typical ceramic/metal electrical feedthrough | 7 |
| Figure 5: Examples of commercial electrical feedthroughs | 8 |
| Figure 6: Gibbs free energy versus pressure for the thermal decomposition of SiO ₂ at 500 K | 15 |
| Figure 7: Estimated leakage rate of helium through amorphous silica and Pyrex at 300 K and 500 K | 17 |
| Figure 8: Schematic of ASTM E 1603: helium leak testing using mass spectroscopy | 24 |
| Figure 9: Schematic of proposed helium leak testing rig | 24 |
| Figure A.1: Approximate thermal expansion of various alloys on heating from room temperature | A5 |

LIST OF TABLES

| | |
|--|----|
| Table 1: Prometheus alternator design specifications | 6 |
| Table 2: Physical properties of selected glasses, glass-ceramics, and alloys | 12 |
| Table 3: Mechanical properties of selected glasses, glass-ceramics, and alloys | 13 |
| Table 4: Minimum thickness required for various insulators based on dielectric breakdown strength, for V _{rms} = 440 V and 10 mm conductor radius | 19 |
| Table 5: Physical and mechanical properties of selected ceramics | 21 |

1.0 INTRODUCTION

The integrity of the alternator electrical feedthroughs was determined to be a critical materials and design issue for the proposed Brayton cycle space nuclear power plant (SNPP) for the Prometheus spacecraft. The alternator electrical feedthroughs were to lead from the reactor gas coolant system (He/Xe gas mixture) into the space vacuum environment. Excessive leakage of the coolant gas, whether through the alternator feedthroughs or elsewhere, was determined to be a potential primary failure mode for the SNPP. Thus, robust, hermetically-sealing electrical feedthroughs were considered essential to the success of the Prometheus mission, as the electrical feedthrough was the sole through-penetration in the coolant system.

Lead responsibility for assessing the materials compatibility and leak integrity of potential electrical feedthrough designs was assigned to the Bettis Advanced Materials Systems Integration (AMSI) group within the Materials Technology (MT) activity, in support of systems design work by the Space Engineering (SE) activity. Potential complications and pitfalls were identified; background literature was researched; potential vendors for the feedthrough assembly were found; and a preliminary testing methodology was proposed. Although the work did not reach the materials or component testing stage, the information contained herein may be useful to groups working with electrical feedthroughs for other space nuclear power plants.

This report describes and addresses the issues facing the electrical feedthrough insulator materials. Some of the properties of potential insulators and conductors for glass/metal, glass-ceramic/metal, and ceramic/metal seal systems are listed, some initial test procedures and protocols are proposed, and some of the feedthrough vendors that could potentially produce the desired product are identified.

2.0 BACKGROUND

2.1 ALTERNATOR DESCRIPTION

The main function of the closed-cycle Brayton turboalternator (or Brayton rotating unit, BRU) in the nuclear propulsion plant for the proposed JIMO spacecraft was to convert thermal-hydraulic energy to mechanical shaft energy, and then to electrical energy. High temperature gas expands through a turbine in the turboalternator, transferring energy to a rotating shaft. The rotating shaft energy drives the alternator, or permanent magnet generator (PMG). The alternator converts mechanical energy to electrical energy for the spacecraft via permanent magnets attached to the spinning rotor, which induce a current in the surrounding stator conductor coils. A model of the proposed turboalternator (as designed by Hamilton Sundstrand) is presented in Figure 1. An exterior view of the turboalternator is presented in Figure 2, depicting the feedthrough leads. Detailed descriptions of the turboalternator can be found in Reference 1.

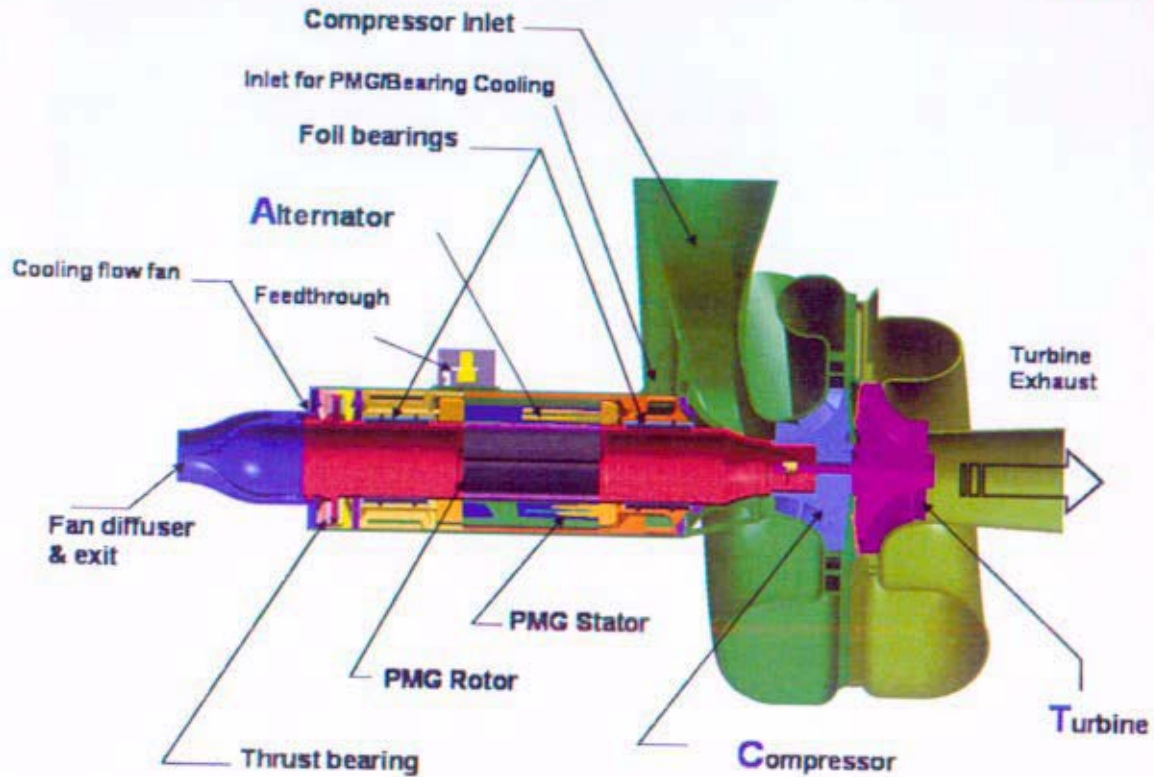


Figure 1. Space Brayton turboalternator conceptual design; from Reference 2.

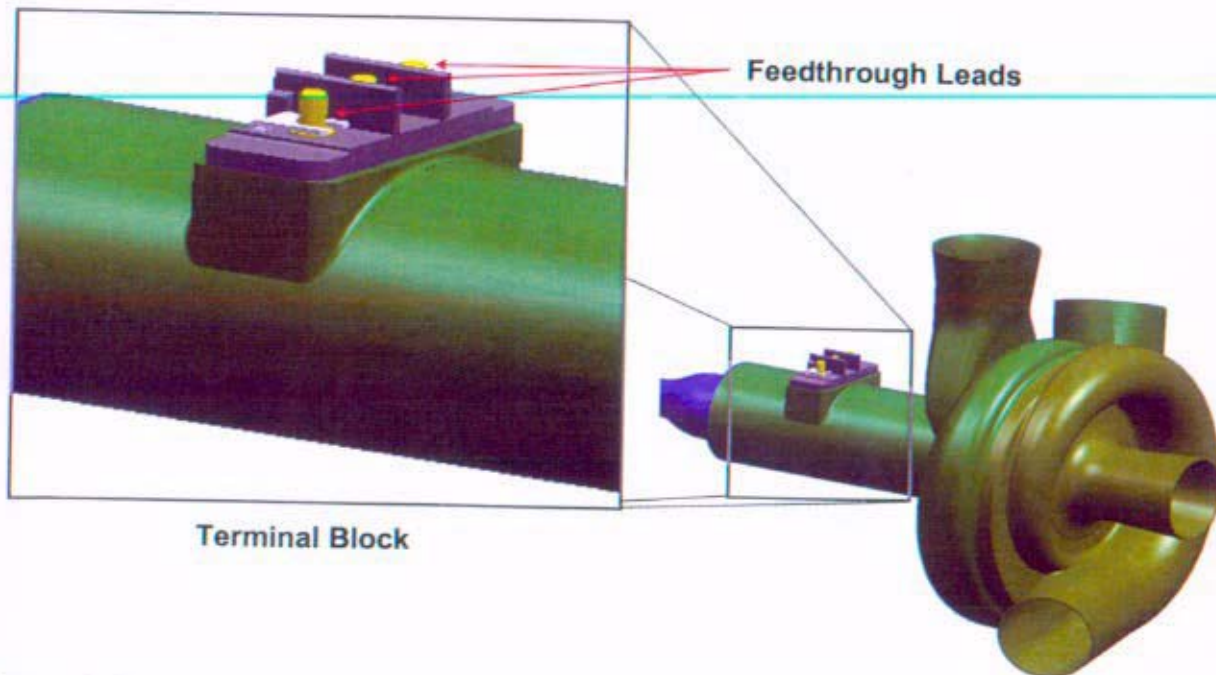


Figure 2. Turboalternator external view depicting feedthrough lead positions; modified from Reference 2.

Expected conditions for a gas-cooled alternator for a Prometheus reactor were determined through design and modeling work performed by the Space Power Program (SPP) section (C. Richardson) and the Fleet Support Operations (FSO) section (E. Pheil) at KAPL. The preliminary design conditions for the alternator are specified in Table 1. According to the initial design, the Brayton power plant, including alternator, was to be located aft of the primary radiation shield. The number of Brayton units to be used on the spacecraft had not yet been specified; therefore more than one turboalternator may have been required [1]. For the case of one Brayton unit on the spacecraft there would have been three leads per terminal block (one for each of three phases) with two terminal blocks per alternator. For two or more Brayton units there would have been only one terminal block per alternator. In general, the number of leads would be equal to the number of feedthroughs required. However, the three leads from one terminal block could have been combined into one single feedthrough.

Table 1. Prometheus alternator design specifications [3,4].

| | |
|---|---|
| Bleedflow gas composition | 78.4 vol% He, 21.6 vol% Xe |
| Bleedflow gas temperature range | 200K to 500K (-100°F to 440°F) |
| Bleedflow maximum gas pressure | 4000 kPa (590 psi) |
| Space vacuum pressure | 1.3×10^{-15} kPa (1×10^{-14} torr) |
| Bleedflow gas flow rate | 0.34 kg/s (2700 lb/hr) |
| Alternator output | Three-phase AC |
| Alternator voltage | 440 Vrms line to line |
| Alternator power | 100 kWe |
| Alternator electrical frequency | 2.25 kHz |
| Average gas leakage rate (max. allowable) | 1×10^{-9} std cc/sec |
| Peak gas leakage rate (max. allowable) | 1×10^{-3} std cc/sec |
| Behind-shield neutron fluence (JIMO) | 6×10^{15} 1MeV Si equivalent n/cm ² |
| Total ionizing dose (JIMO) | 500 Mrad |

2.2 ELECTRICAL FEEDTHROUGH GAS LEAKAGE CONCERNS

The function of the alternator electrical feedthrough is to pass high voltage from the alternator to the spacecraft electrical system through the alternator coolant fluid pressure boundary. The feedthrough is intended to hermetically seal the coolant pressure boundary from the vacuum of space. A simplified schematic of the electrical feedthrough assembly concept portrayed herein is presented in Figure 3, and a commercial schematic of the components and assembly of a typical ceramic/metal seal is displayed in Figure 4. The conductors running through the feedthroughs were to be joined to wires connecting the electrical wiring systems of the alternator to the rest of the spacecraft. The feedthrough housing, or "body," would be attached and hermetically welded to the pressure boundary, or coolant piping system. The feedthrough insulator would electrically insulate the conductors from the body, while also providing a hermetic seal. Examples of existing electrical feedthrough assemblies are provided in Figure 5. The feedthroughs in Figure 5 represent those utilizing ceramic/metal and polymer gland sealants.

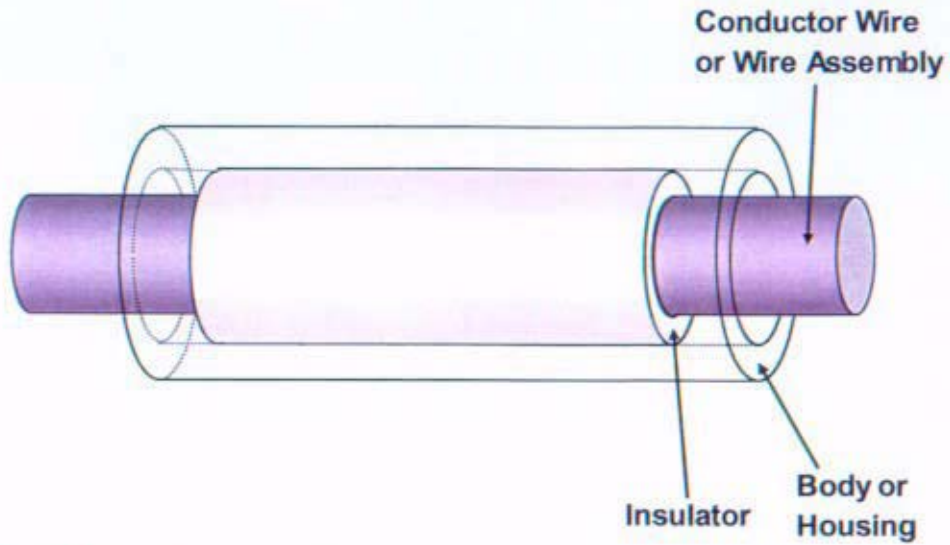


Figure 3. Simplified schematic of electrical feedthrough assembly.

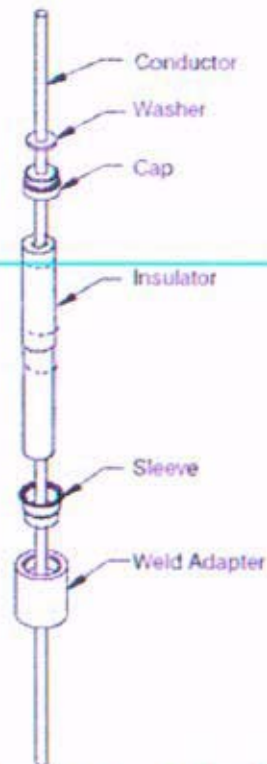


Figure 4. Schematic of components and assembly of a typical ceramic/metal electrical feedthrough; from Reference 5.

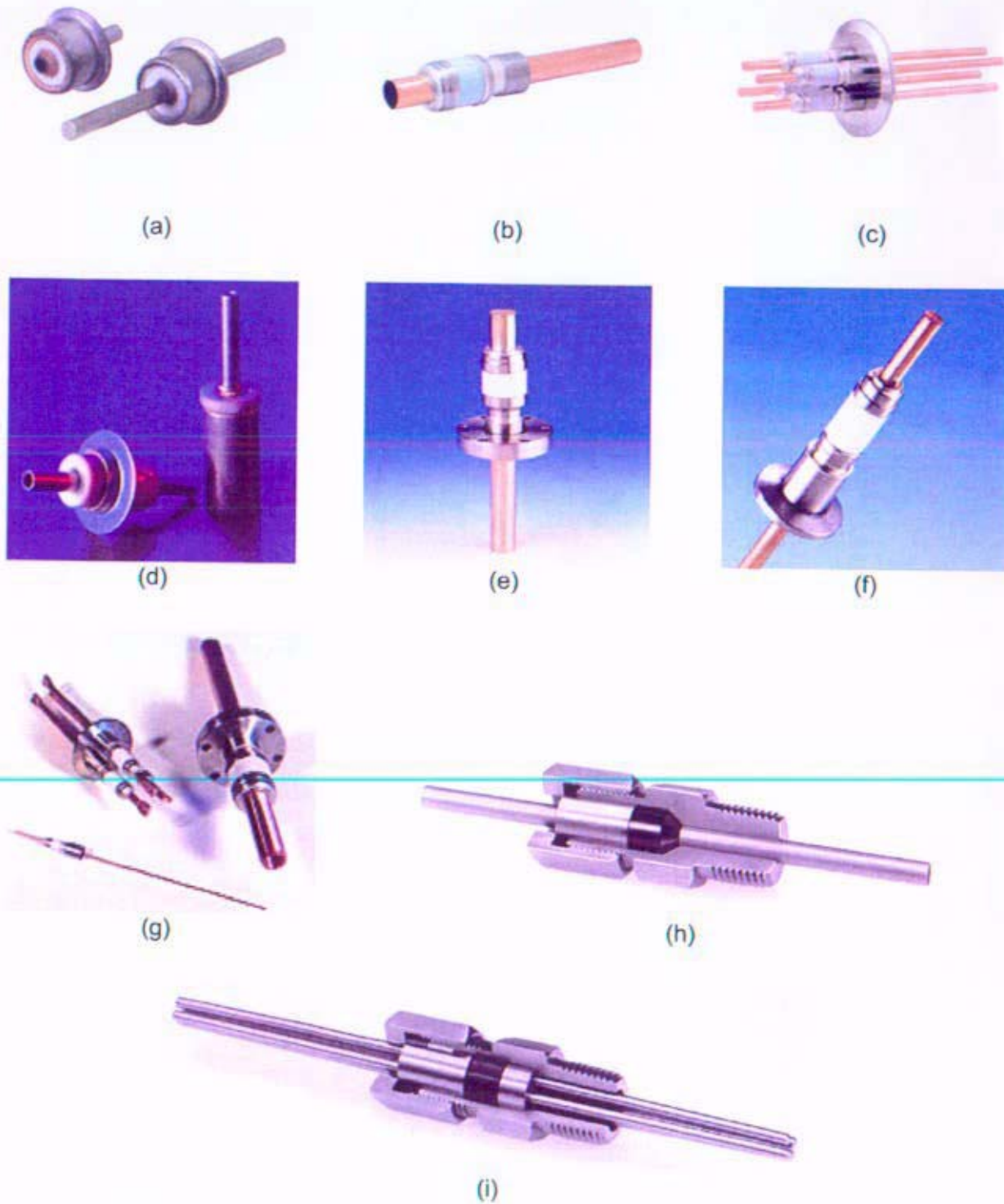


Figure 5. Examples of commercial electrical feedthroughs: (a-c) CeramTec ceramic/metal feedthroughs [5]; (d) Latronics ceramic/metal feedthroughs [6]; (e-f) MDC ceramic/metal feedthroughs [7]; (g) SST ceramic/metal feedthroughs [8]; (h-i) Conax polymer gland feedthroughs [9].

The design for the Prometheus Jupiter Icy Moons Orbiter (JIMO) mission required a minimum maintenance-free alternator lifetime of 15 years. The feedthrough length was predicted to be 70 mm with a conductor radius of about 10 mm (~20 mm diameter). Notionally, five Watts of electrical power losses were allowed in the cable as it passed through the feedthrough. The initial choice of feedthrough housing and conductor material was Inconel 625 on the basis of overall material compatibility with the proposed coolant piping system [10]. However, this choice was subject to change based upon research into the feedthroughs. Materials considered for the coolant piping system included wrought nickel-based superalloys such as PE16, Haynes 230, Inconel 617, and Hastelloy X [1].

A paramount concern for the electrical feedthroughs was the loss of helium and xenon gas from the cooling system. The maximum time-averaged single feedthrough gas (He/Xe) leakage rate was preliminarily defined as 1×10^{-9} std cc/sec, the vacuum industry standard, over the 15 year lifetime of the alternator. The peak instantaneous maximum gas leakage rate for a single feedthrough was preliminarily defined as 1×10^{-3} std cc/sec (see Reference 3 for details). Leakage of coolant in excess of these rates was defined as failure for a test feedthrough. The most likely coolant leakage path was judged to be that through the electrical feedthroughs, welds, and joints in the system, especially through microcracks, pores, and other defects in these parts. For fully-dense and defect-free parts, the primary expected leakage source would be atomic diffusion driven by concentration gradients in accordance with Fick's Law. Based on simplified estimates for bulk diffusion through stainless steel, less than a 1% pressure loss is projected over the 15 year mission [11]. Similar extrapolations were made for bulk diffusion through refractory metals. Therefore, He/Xe bulk diffusion through dense metal components was determined not to be an important life-limiting process for the coolant system. However, He/Xe leakage through metal-to-ceramic, metal-to-glass, and metal-to-polymer joints in electrical feedthroughs is of concern. Thus, He/Xe containment would have required a near-perfect, hermetic insulator/conductor system impervious to the mechanical, chemical, and electrical rigors of the mission.

Concerns regarding the longevity of the seals included radiation exposure (including, for example, the (n,α) reaction in boron-containing materials), tensile stress development, thermal cycling and fatigue, vibration and mechanical fatigue, creep, and chemical contamination (due, for example, to interdiffusion of impurities or reactions with fission products) [12,13]. The primary issues for the feedthroughs were the integrity of the conductor-to-insulator seal, the insulator-to-body seal, the sealant itself, and the body weld joints [12].

Given the stated conditions, Bettis MT-AMSI endeavored to identify a suitable feedthrough insulator system capable of retaining its integrity over the 15 year lifespan of the JIMO mission. Preliminary research efforts explored commercially available hermetic electrical feedthroughs. Potential vendors were identified, researched, and consulted. Many commercial hermetic electrical feedthroughs are based on polymeric sealants. The thermal and radiation resistance properties of polymer-sealed feedthroughs were judged to be generally inadequate to survive a 15-year mission. Therefore, the bulk of the research effort into the electrical feedthrough insulator materials for the Prometheus spacecraft was devoted to technologies based on glass, glass-ceramic, and ceramic insulators.

3.0 GLASS/METAL AND GLASS-CERAMIC/METAL SEALS

Glass is defined as an amorphous solid with no long-range order. Glasses are in a thermodynamically metastable state. They form from a melt without crystallization because their high viscosity at the melting point limits their ability to rearrange for crystallization [14]. Examples of glass network forming oxides include Si, Ge, B, P, and As. Cations, especially alkali and alkaline earth metals such as Na, K, Mg, Ca, and Ba, can be incorporated into silicate glasses to provide additional oxygen ions to modify the network of silica tetrahedra. These are called network modifiers. Intermediate cations with slightly higher valence than the modifiers (e.g. Al, Ti, Zn, Pb) can act as both network formers and modifiers [15]. Neither modifying oxides nor intermediate oxides are able to form a glass by themselves at conventional cooling rates.

Glass/metal seals are a well-established, versatile technology. Glass/metal seals were developed well over a century ago and have many applications including hermetic seals in light bulbs, electronics, batteries, and weapons [16]. Glass/metal sealing is typically performed through a fusion bonding technique in which glass is heated into the molten state and is chemically bonded to the metal substrate through wetting and other chemical processes. These seals are simple and relatively inexpensive to manufacture. The molten glasses can be processed by any of a number of techniques, including casting, rolling, blowing, extrusion, and molding [14]. Cleaning of the metal and glass parts must be performed to enhance bonding characteristics. Roughening of the metal surface may also be performed (e.g. by sandblasting) to induce a degree of mechanical adherence. Annealing of the glass must be performed carefully to avoid large thermal strains within the glass. The importance of proper annealing increases as the thickness of the glass increases. Glass/metal seal processing techniques vary between manufacturers and are often proprietary.

The coefficient of thermal expansion (CTE) of glasses can be modified (via compositional changes) to match the CTE of many different metals, thus reducing thermally induced stresses. At moderate temperatures and mechanical loads, glass seals are capable of providing reliable long-term service. But at high temperatures, high loads (especially tensile), and in certain environments, glass/metal seals are not suitable. Also, glass is generally more permeable to diffusing gases, such as helium, than ceramics and other materials. These factors could limit the applicability of glass-insulated electrical feedthroughs for the Brayton alternator(s) for Prometheus.

A promising alternative to glass/metal seals for the Prometheus alternator feedthrough are glass-ceramic/metal seals. Glass-ceramic/metal seals offer many of the advantages of glass/metal seals such as straightforward manufacturability, while also providing much of the superior mechanical strength, greater chemical stability, and better electrical insulating properties of ceramics. More importantly, glass-ceramics provide a much greater range of CTEs than glasses or other ceramics by control of the crystallization process [17]. CTE values for glass-ceramics can range from slightly negative to over $20 \times 10^{-6}/K$ [14].

While glass-ceramics often have enhanced properties and better chemical resistance than glasses, their processing is more complex and generally requires both sealing (high-temperature) and highly-controlled crystallization (intermediate temperature) thermal cycles. The small-grained crystalline inclusions (typically smaller than $1 \mu m$) significantly alter and usually enhance the properties of the material. The crystallinity in glass-ceramics may exceed 90% [14]. However, the forming of glass-ceramics (by, e.g. casting, rolling, molding, and

powder sintering) is still generally easier than for ceramics; and complex shapes can be formed by flowing molten glass into a preform, or by forming the glass component prior to the sealing and crystallization steps. During processing, the molten glass first wets the metal substrate and forms a strong chemical bond between the glass and metal. The amorphous glass is then partially devitrified and crystallized by the heat treatment and results in a tough glass/polycrystalline composite. Glass-ceramics are often a good alternative to both glasses (properties) and ceramics (ease of processing and property tailoring) as sealing materials. Further details of the processing and design considerations for glass/metal and glass-ceramic/metal seals are provided in Appendix A.

Lithium-silicate glass-ceramics (about 67-71% SiO_2 , 20-25% Li_2O , and other additives) are especially strong at higher temperatures and have been utilized as hermetic seals for nickel-based power feedthroughs [16]. Significant work has been performed in the area of lithium-silicate glasses [18]. This work has developed appropriate processing steps and identified the ceramic phases formed as Li_2SiO_3 , $\text{Li}_2\text{Si}_2\text{O}_5$, and cristobalite (SiO_2), which are nucleated by Li_3PO_4 or LiPO_4 crystallites. Temperatures of up to 1075-1475 K (1475-2200°F) are typically used during the sealing process, with somewhat lower temperatures for subsequent nucleation and crystallization steps. These glass-ceramics are potentially useful for the Brayton electrical feedthrough with a Ni-based superalloy conductor.

Reactions between the glass and the metal and crystallization of the glass during glass-ceramic/metal sealing can adversely affect the resulting microstructure, including a reduction in the amount of glass-ceramic formed near the interface and the creation of concentration gradients and residual stresses at the interface [14]. High residual stresses are a potential issue with glass-ceramic/metal seals due to potential concentration gradients of the crystalline ceramic phases within the glass. Thus, the chemistry of the system across a large temperature range must be well characterized before being used for seals for critical components.

3.1 MECHANICAL INTEGRITY OF GLASS/METAL SEALS

Several mechanical properties are of interest in this application. Some of the physical and mechanical properties of glasses, glass-ceramics, and alloys are presented in Table 2 and Table 3. For mechanical integrity of glass/metal seals, the materials must bond strongly (good adherence); all material phases must have sufficient strength and toughness to avoid crack formation and propagation; the thermal expansion properties of the phases must be somewhat similar to avoid large thermal stresses; and all phases must be resistant to thermal shock. The material properties must not degrade severely over time, therefore mechanical fatigue, creep, and change in properties due to chemical reactions must be limited.

The glasses used for sealing applications are specific to the metal to which they are bonded in terms of both chemistry and CTE matching. As shown in Table 2, the CTEs of metals and glasses are usually significantly dissimilar, with metals usually having significantly larger CTEs than glasses. For glass/metal seals, Tomsia et al. state that the CTEs of the materials should be within 10% of each other over the range from the glass transition temperature (or set point) of the glass to the lowest usage temperature. Diffusion of metal oxides into the glass can create a graded CTE in the glass that improves the quality of the seal by reducing mismatch stresses [14].

Table 2. Physical properties of selected glasses, glass-ceramics, and alloys [19-34].

| Glasses | Glass Trans. Temp., T_g (K) | Density (g/cm^3) | CTE $\alpha \times 10^{-6}$ 293-573K (K^{-1}) | Thermal Conductivity 300K (W/m·K) | Electrical Resistivity $\Omega \cdot m$ (300K) | Electrical Resistivity $\Omega \cdot m$ (523K) |
|---|-------------------------------|----------------------|---|-----------------------------------|--|--|
| 7052 Borosilicate ^g | ~710 | 2.27 | 4.6 | - | $>10^{17}$ | 1.6E+07 |
| 8248 Borosilicate ⁱ | 718 | 2.12 | 3.1 | - | - | 1.0E+10 |
| 0080 Soda-lime ^{g,a} | ~750 | 2.47 | 9 | 1.7 | 2.5E+10 | 2.5E+04 |
| Soda-silica (60% SiO ₂) ^j | - | - | 16.5 | - | - | - |
| Soda-silica (92% SiO ₂) ^j | - | - | 7.7 | - | - | - |
| 8250 Glass ⁱ | 763 | 2.28 | 5 | - | - | 1.0E+08 |
| 8253 Glass ⁱ | 1058 | 2.65 | 4.7 | - | - | - |
| 8421 Glass ⁱ | 798 | 2.59 | 9.7 | - | - | 1.3E+06 |
| 8487Suprax Glass ⁱ | 828 | 2.32 | 4.1 | - | - | 3.2E+05 |
| 7940 Fused Silica (quartz) ^g | ~1230 | 2.2 | 0.56 | 1.4 - 2.0 | $>10^{17}$ | 2.5E+10 |
| Glass-Ceramics | | | | | | |
| 9606 Glass-Ceramic ^g | - | 2.6 | 5.70 | - | 5.0E+14 | 1.0E+08 |
| 9608 Glass-Ceramic ^g | - | 2.5 | 0.4 - 2 | - | 2.5E+11 | 1.3E+06 |
| Metals | Melting Point (K) | Density (g/cm^3) | CTE $\alpha_{ave} \times 10^{-6}$ 300K (K^{-1}) | Thermal Conductivity 300K (W/m·K) | Electrical Resistivity $\Omega \cdot m$ (300K) | |
| Inconel 625 ^{a,b,c} | 1560-1625 | 8.4 | 12.8 | 9.8 | 1.3E-06 | |
| Inconel 600 ^{a,b,c} | 1630-1705 | 8.4 | 13.3 | 14.8 | 1.0E-06 | |
| Kovar ^k | 1450 | 8.4 | 5.2 | 17.3 | 4.9E-07 | |
| Alloy 42 ⁿ | 1713 | 8.1 | 6.0 | 10.7 | 7.0E-07 | |
| Alloy 52 ⁿ | 1698 | 8.3 | 10.0 | - | 4.3E-07 | |
| NILO 48 ^o | 1723 | 8.2 | 8.7 | 16.7 | 4.7E-07 | |
| 304 SS (annealed) ^e | - | 8.0 | 17.2 | 16.2 | 7.2E-07 | |
| 316 SS (annealed) ^e | - | 8.0 | 15.9 | 16.2 | 7.4E-07 | |
| Alumel ^p | 1588-1663 | 8.5 - 8.7 | 16.8 | 30 - 32 | 3.1E-07 | |
| Chromel ^p | 1693 | 8.5 | 17.2 | 19.0 | 7.1E-07 | |
| Constantan ^o | 1498-1573 | 8.9 | 14.9 | 19.5 | 5.2E-07 | |
| W ^{e,h} | 3683 | 19.3 | 4.5 | 155 | 5.3E-08 | |
| Mo ^{e,h} | 2883 | 10.2 | 4.9 | 142 | 5.2E-08 | |
| Ti ^{e,h} | 1941 | 4.5 | 8.4 | 16.0 | 4.2E-07 | |
| Pt ^h | 2042 | 21.5 | 9.1 | 71.1 | 1.1E-07 | |
| Ni ^h | 1728 | 8.90 | 16.6 | 82.9 | 6.8E-08 | |
| Cu ^h | 1358 | 8.93 | 17.5 | 398 | 1.7E-08 | |
| Ag ^h | 1235 | 10.49 | 20.6 | 428 | 1.5E-08 | |
| Al ^h | 933 | 2.70 | 27.4 | 247 | 2.6E-08 | |
| 7052 Borosilicate = 64% SiO ₂ , 8% Al ₂ O ₃ , 19% B ₂ O ₃ , 3% BaO | | | 8487Suprax = Schott sealing glass for W | | | |
| 8248 = Schott borosilicate insulating glass | | | 7940 Fused Silica = 99.9% SiO ₂ | | | |
| 8250 = Schott sealing glass for Fe-Ni-Co and Mo | | | 9606 Glass-Ceramic = 56% SiO ₂ , 20% Al ₂ O ₃ , 15% MgO | | | |
| 8253 = Schott alkaline-earth aluminosilicate sealing glass for Mo | | | 9608 Glass-Ceramic = 70% SiO ₂ , 18% Al ₂ O ₃ , 3% Li ₂ O, 3% MgO | | | |
| 8421 = Schott sealing glass for NiFe45 and compression seals | | | | | | |

(table continued next page)

| | |
|---|---|
| a) Everhart, <i>Engineering and Properties of Nickel...</i> | k) High Temp Metals, Kovar product technical data sheet |
| b) ASM <i>Specialty Handbook: Heat-Resistant Materials</i> | l) Mizuhara and Oyama, "Ceramic/Metal Seals" |
| c) Mankins and Lamb, "Nickel and Nickel Alloys" | m) Insaco, Inc. product data |
| d) Robie, et al., <i>Thermodynamic Properties of Minerals...</i> | n) H. Cross Company, product data |
| e) Callister, <i>Materials Science and Engineering: An Introduction</i> | o) Special Metals, product data |
| f) Kirk-Othmer <i>Encyclopedia of Chemical Technology, Vol. 5</i> | p) Goodfellow, product data |
| g) Kirk-Othmer <i>Encyclopedia of Chemical Technology, Vol. 11</i> | q) <i>CRC Handbook of Chemistry and Physics</i> |
| h) ASM <i>Handbook Volume 2 – Properties and Selection...</i> | r) Kingery, et al., <i>Introduction to Ceramics</i> |
| i) Schott Technical Glasses product data | s) Cengel and Turner, <i>Fundamentals of Thermal-Fluid Sciences</i> |
| j) Morey, <i>The Properties of Glasses</i> | |

Table 3. Mechanical properties of selected glasses, glass-ceramics, and alloys [19-34].

| Glasses | Elastic Modulus, E 300K (GPa) | Poisson's Ratio | Knoop hardness HK_{100} | Fracture Toughness ($MPa \cdot m^{1/2}$) | |
|---|---------------------------------|-----------------|---------------------------------------|--|---------------------|
| 7052 Borosilicate ^g | 57 | 0.22 | 375 | - | |
| 8248 Borosilicate ⁱ | 44 | 0.22 | - | - | |
| 0080 Soda-lime ^{g,e} | 69 | 0.22 | 465 | 0.75 | |
| 8250 Glass ^l | 64 | 0.21 | - | - | |
| 8253 Glass ^l | 83 | 0.23 | - | - | |
| 8421 Glass ^l | 74 | 0.22 | - | - | |
| 8487 Suprax Glass ^l | 66 | 0.20 | - | - | |
| 7940 Fused Silica (quartz) ^g | 73 | 0.16 | - | - | |
| Glass-Ceramics | | | | | |
| 9606 Glass-Ceramic ^g | 118 | 0.24 | 657 | - | |
| 9608 Glass-Ceramic ^g | 86 | 0.25 | 593 | - | |
| Metal | Elastic Modulus, E 300K (GPa) | Poisson's Ratio | Yield Strength, σ_y 300K (MPa) | Annealed UTS, σ_f 300K (MPa) | Elongation 300K (%) |
| Inconel 625 ^{a,b,c} | 208 | 0.31 | 290 - 520 | 720 - 970 | 50 |
| Inconel 600 ^{a,b,c} | 214 | 0.29 | 170 - 345 | 550 - 690 | 45 |
| Kovar ^k | 138 | - | 345 | 517 | 30 |
| Alloy 42 ⁿ | 145 | 0.25 | 276 | 496 | 35 |
| Alloy 52 ⁿ | 166 | 0.29 | 207 | 517 | 30 |
| NILO 48 ^o | 160 | - | 260 | 520 | 43 |
| 304 SS (annealed) ^e | 193 | 0.30 | 205 | 515 | 40 |
| 316 SS (annealed) ^e | 193 | 0.30 | 205 | 515 | 40 |
| Alumel ^p | - | - | - | 550 - 780 | <44 |
| Chromel ^p | 186 | - | - | 620 - 780 | <44 |
| Constantan ^o | 162 | - | - | 400 - 590 | <45 |
| W ^{e,h} | 400 | 0.28 | 760 | 960 | 2 |
| Mo ^{e,h} | 320 | 0.32 | 500 | 630 | 25 |
| Ti ^{e,h} | 103 | 0.34 | 140 | 235 | 54 |
| Ni ^h | 207 | 0.31 | 59 | 317 | 30 |
| Cu ^h | 128 | 0.34 | 33 | 209 | 60 |
| Ag ^h | 71 | 0.37 | - | 125 | - |
| Al ^h | 62 | 0.33 | 15 - 20 | 40 - 50 | 50 - 70 |

* References are the same as in Table 2.

There are two categories of glasses, hard and soft. Hard glasses, like borosilicates and aluminosilicates, have higher working temperature ranges (1275-1575 K) and lower CTEs (less than $5 \times 10^{-6}/K$). In contrast, soft glasses such as common soda-lime silicate glass have lower working temperatures (1075-1275 K) and higher CTEs (greater than $5 \times 10^{-6}/K$). Therefore, soft glasses generally have better CTE matches with metals than hard glasses [14]. Other mechanical properties of soft glasses may not be satisfactory, such as low electrical resistivity, strength, toughness, or thermal shock resistance. In terms of thermal shock resistance, estimates of the thermal stresses in glasses include 75-80 MPa of stress for a 100 K (180 F°) temperature difference across silica glass, 22 MPa of stress in a low-expansion borosilicate glass, or 10 MPa in vitreous silica [35].

The tensile strength of bulk glass (~ 1-8 MPa) is generally about 10-20 times less than the compressive strength of the glass [14]. Because of this, residual tensile stresses in a component should be minimized. Induced compressive stresses can counteract tension and can be obtained by different tempering methods, including by controlling the cooling rate after fusion (i.e. by forming a rigid layer on the surfaces while the center of the glass is still plastic).

Fracture may occur at any region of a glass/metal seal including at junctions between the metal and metal oxide layers, within the metal oxide, at the metal oxide/glass interface, or within the glass [36]. However, failure rarely occurs in the metal to metal oxide interface. Fracture within the metal oxide itself is not common because the metal and its oxide frequently have reasonable CTE matching and inherently strong chemical bonding. Fracture in the metal oxide layer becomes important when the oxide layer is too thick and is vulnerable to flaws [36]. Due to their residual stresses and high density of flaws, the interface zone between the metal oxide and the glass is often the origin of fracture in glass to metal seals. The stress and flaws at the interface arise from chemical reactions, preexisting flaws at the oxide surface, and CTE mismatch. Properties such as elastic modulus, CTE, and glass transition temperature often deviate significantly near the interface compared to the bulk values, making interface behavior extremely difficult to accurately predict [14]. Once cracking is initiated in the interface region, cracks will propagate either at the interface or within the glass, as described in the Appendix section "Seal Design," page 4.

Because the strength of glass/metal seals is often dependent on the number of random flaws at the interface or in the glass, the strength of glass/metal seals is determined by statistical processes [36]. Considering this and the fact that the stress levels in glass/metal seals are highly dependent on geometry, numerous experiments must be performed on prototypical components to demonstrate component reliability.

3.2 CHEMICAL INTEGRITY OF GLASS/METAL SEALS

Possible chemical integrity issues for glass/metal seals include interfacial reactions, gas evolution from the metal, bubble formation in the glass, out-gassing of the glass into the vacuum of space, chemical attack of the glass by fission products, and loss of coolant gas through the glass via chemical diffusion.

The diffusion of species across the joint interface is one of the main issues of concern in terms of the seal stability. Because chemical reactivity is thermally induced, prolonged exposure of the materials to elevated temperature (~500 K) must be considered. While diffusion and/or reaction of most ceramic, glass, and metal alloy joint components may be relatively slow at

these temperatures, the diffusion and reactions over the 15+ year lifetime of the component could be significant. One potential pitfall is the creation of new phases near the interface because of changes in the concentration of the constituents. For example, these new phases may be brittle, weak, or electrically conductive; or they may produce CTE incompatibilities at the interface. Furthermore, diffusion of chemical species into or out of a material may significantly degrade the material properties. The long-term chemistry of the bonded materials must be fully characterized before use in the Prometheus spacecraft.

Gas evolution from the metal and subsequent bubble formation in the glass seal is a serious issue which can greatly degrade the mechanical integrity and hermeticity of seals. However, proper processing techniques can eliminate this problem. Chemical decomposition and evaporation of glass is another possible issue with glass/metal seals. As shown in Figure 6 (based on FactSage™ thermodynamic calculation), crystalline quartz, which is only slightly more thermodynamically stable than amorphous silica, is not susceptible to gaseous decomposition in the temperature and pressure regime of the present application. It is anticipated that the silica in other silicate-based glasses and glass-ceramics will exhibit similar thermal stability, and thus decomposition and evaporation of silica from the glass should not be a limiting issue.

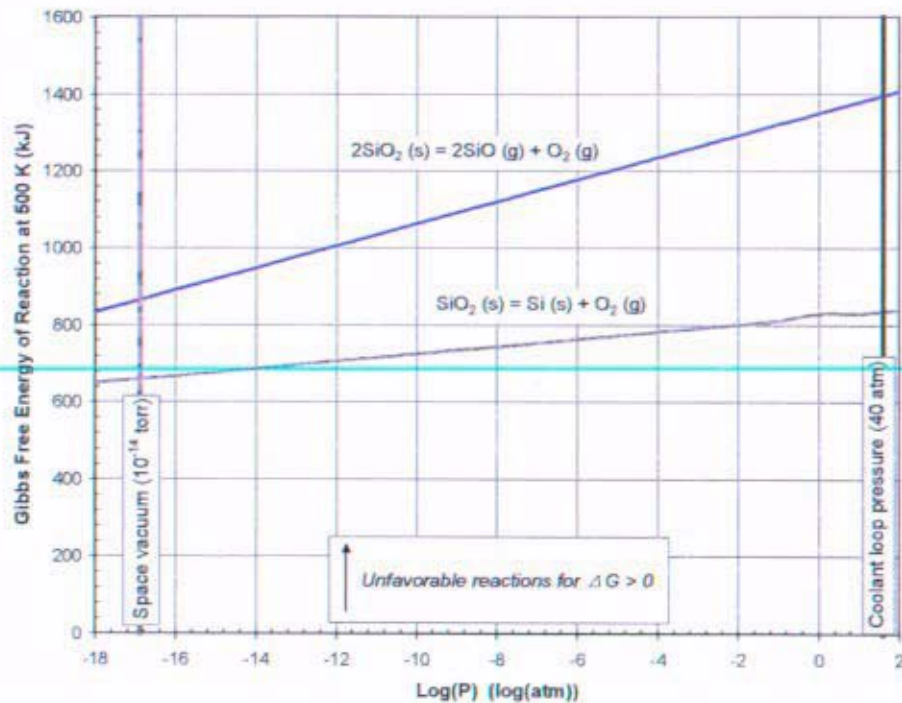


Figure 6. Gibbs free energy versus pressure for the thermal decomposition of SiO_2 at 500 K.

While the vaporization of silica itself should be a minor concern, chemical components of some glasses are more susceptible to volatilization. These include the alkali metals, halogens, lead, and boron; and the volatility generally increases with increasing atomic number [35]. Volatilization is accelerated with an increase in temperature and with a decrease in vapor pressure, or a lower partial pressure of the chemical species. The evaporation of individual

components of the glass could be a potential problem over the 15-year lifespan of this application, especially any portion of the glass exposed to elevated temperature and/or the vacuum of space. Tests would have to be performed to verify that the glass composition would not significantly change under the extended period at elevated temperature and vacuum.

The extent of glass or glass-ceramic corrosion in a glass/metal seal system remains unknown. Reactions of the feedthrough component with various potential chemical contaminants in the system would have to be researched and tested before implementation. Fission product contaminants from fuel cladding failure (e.g. in the coolant stream) are chemicals of concern, especially common fission products such as cesium, iodine, and tellurium. Calculations performed with the thermodynamic chemistry software FactSage™ showed that the free energies of reaction for the reduction of silica to SiO or Si by cesium, iodine, and tellurium, over the range of temperatures and pressures expected, were all highly positive. Therefore, silica redox reactions with common fission products are unlikely due to their positive reaction free energies. However, fission product chemicals may dissolve into the glass and modify, for example, the glass's mechanical, electrical, or gas permeability characteristics. The effect of fission products on glass is not completely understood at this time and should be further investigated.

The gas permeability of the glass/metal seal is extremely important for the application described herein. In order to conserve the helium/xenon cooling gas, the maximum gas leakage rate from the feedthrough is expected to remain below an average rate of 10^{-9} standard cc/sec; and also below an instantaneous maximum rate of 10^{-3} standard cc/sec (however, these numbers could change significantly after process design refinement). There are two possible leakage mechanisms including gas diffusion through defects (e.g. cracks and macroscopic porosity), which can be controlled through proper design and processing of the glass to metal seal; and diffusion of gas molecules through the solid structures.

Excluding surface reactions, gas permeability, or flux, through solid bodies is influenced by gas solubility and molecular diffusion. Solubility is typically the rate limiting factor in metals and other solids. Diffusion may be the limiting factor in solids with open structures and high gas solubility such as glass. Diffusion of gas through glass is inversely proportional to the size of the diffusing species and directly proportional to the degree of openness in the glass structure. Smaller gas molecules can diffuse through smaller pathways in the structure; and thus lower dilation energies are required for diffusion. Therefore, helium is the most mobile gaseous species in glass (as hydrogen and other diatomic gases do not dissociate in glass) [35]. Gas leakage (flux), J , and permeation, p , via molecular diffusion are given by the following equations.

$$J = p(\Delta P) / \delta$$
$$p = p_0 \exp(-Q / RT) = \sigma D$$

where p_0 is the permeation constant, ΔP is the pressure differential, δ is the diffusion length, Q is the permeation activation energy, T is the absolute temperature, R is the universal gas constant, σ is the Henry's law solubility constant, and D is the diffusion coefficient [37]. The initial addition of glass modifiers such as lithium and sodium in silicate glasses can significantly increase the permeation activation energy and decrease the gas diffusivity, primarily due to modifier cation occupation of interstices [38]. However, changes in structure result in diffusivity minima with increases in modifier concentration. For example, at 525 K (480°F), the amount of Na₂O for minimum helium diffusivity is 19-20 mol%. The helium diffusivity increases by an order of magnitude below 7% and above 33% Na₂O [35].

Figure 7, calculated from the equations above and data from Reference 37, shows the He gas permeation through amorphous silica and Pyrex glass as a function of insulator radial thickness. From these calculations, it is apparent that the leakage of He via diffusion in defect-free silicate glasses borders on the preliminary acceptable leakage rate (10^{-9} std cc/sec) at 500 K (440°F), depending heavily on the type of glass. Diffusion-based leakage processes alone may exceed the preliminary leakage rate limits if the glass radial thickness is too large. The permeation of xenon through solids should be much lower than that of helium because of the difference in size of atoms. Significant selective loss of helium could change the coolant gas composition, affecting the coolant performance, and should be considered in design calculations.

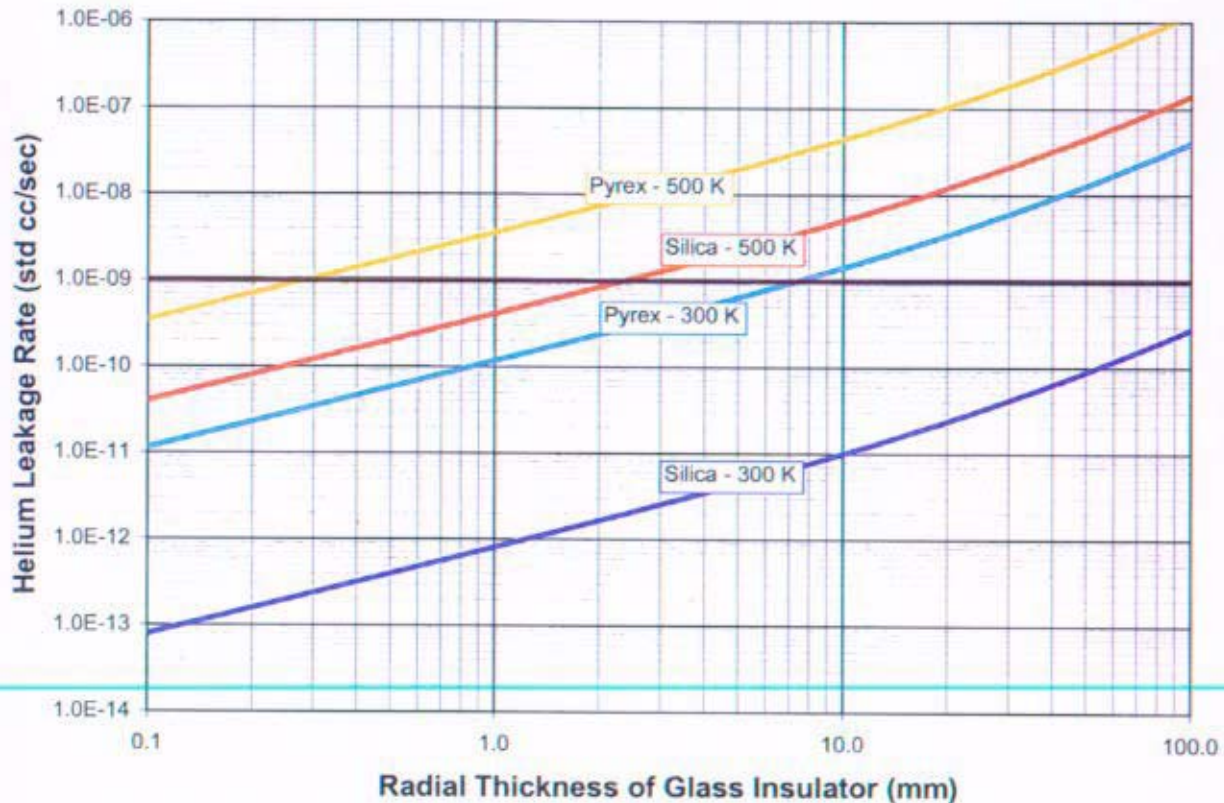


Figure 7. Estimated leakage rate of helium through amorphous silica and Pyrex at 300 K and 500 K (10 mm radius wire, 70 mm glass length and diffusion pathway).

Diffusion of glass cations is important in terms of chemical reactivity, electrical conductivity, and glass properties. The diffusion of ions with valence greater than 1 is usually very low. Diffusion of monovalent cations generally varies inversely with cation size [35]. Both diffusion and chemical reactivity are thermally activated processes.

Chemical reaction analyses of potential glasses with system contaminants would have required knowledge of the expected concentration of contaminants in the environment, which were unknown at this stage of development.

Radiation resistance of glasses and ceramics is an important chemical property for this materials application. The neutron radiation exposure predicted for this application is orders of

magnitude lower than the general dose limits for the materials, which are about 10^{20} neutrons/cm² for glasses and 10^{21} neutrons/cm² for oxide, nitride, and carbide ceramics. The ionizing radiation dose limits for glasses ($\sim 10^{10}$ rads) and ceramics ($\sim 10^{11}$ rads) also generally exceed the expected mission exposure (5×10^8 rads). Metals typically have even higher dose limits and are not greatly affected by ionizing radiation [39]. Materials containing boron could be problematic in neutron irradiation environments. The large neutron capture cross section associated with the (n, α) reaction in B¹⁰, which produces lithium (known to be deleterious in many glasses) and helium, raises clear concerns for any application of a boron-containing compound in a neutron environment. Extensive radiation testing would be expected before any feedthrough was employed for the Prometheus application.

3.3 ELECTRICAL INTEGRITY OF GLASS/METAL SEALS

It is expected that as long as the seal is designed and manufactured correctly, proper electrical insulation between the feedthrough wire(s) and body will be maintained. Proper design ensures that the insulator physically separates the wires from the feedthrough body (and from other wires, if necessary) along the length of the feedthrough with sufficient thickness to prevent dielectric breakdown. Electrical power (I^2R) losses in the conductor and current losses through the insulator would ideally be minimized to maximize the electrical efficiency. However, for most alloy/insulator combinations, the electrical losses through the feedthrough would likely be negligible compared to the losses in the windings and stator core.

The dielectric breakdown strength of the insulator is probably the most important electrical property of the insulator for this application. If the dielectric strength is exceeded by the electric field in the insulator (which results from the voltage imposed on the conductor), the electrical system will short circuit. For concentric cylinders, the maximum voltage, V_{\max} , that can be withstood by an insulator of dielectric breakdown strength $E_{\text{breakdown}}$ is:

$$a \ln\left(\frac{b}{a}\right) E_{\text{breakdown}} = V_{\max}$$

where a is the radius of the conductor and b is the outer radius of the insulator. The minimum thicknesses, $b-a$, of various insulating materials are shown in Table 4 for $V_{\max} = V_{\text{rms}}\sqrt{2} \approx 620$ Volts and $a = 10$ mm. For ranges of dielectric strength values, the low value of the strength was used in the calculations.

It is expected from the data in Table 4 that the thickness of the insulator required to prevent dielectric breakdown would be about 0.1 mm or thinner. However, in practice a much thicker insulator would be used. For example, local electrical stress concentrations can arise at surface irregularities such as wire asperities and cracks in the insulator. These greatly reduce the applicable dielectric strength of the insulator from that of the theoretical value. Other microstructural defects such as porosity at grain boundaries in polycrystalline ceramics have been shown to decrease the apparent dielectric strength of the ceramics, and would also be expected to apply to porosity in glasses. This especially may be a concern with potential radiation-induced porosity in the insulator. Therefore, significant design allowances must be made, especially with the long maintenance-free lifetime requirement and irreparable nature of this application.

Electrical conductivity of most glasses results from ionic transport of cations (usually monovalent cations). Depending on the concentration of monovalent cations in the glass, glasses can act as insulators or conductors. For the Prometheus application, the insulator must

be highly electrically resistive. The electrical conductivity of the insulating material must not increase greatly over the lifetime of the alternator. Therefore, possible chemical reactions within the system must be well-characterized. Migration of conductive metal into any radial cracks within the glass or ceramic insulator must be minimized. Surface migration of metal into cracks in the insulator has been characterized for many systems; and is often associated with the presence of water or halogens [40].

Table 4. Minimum thickness required for various insulators based on dielectric breakdown strength, for $V_{rms} = 440$ V and 10 mm conductor radius.
(Data obtained from Reference 33 unless otherwise noted).

| Material | Dielectric Strength (kV/mm) | Min. Dielectric Radial Thickness (μ m) |
|--|-----------------------------|---|
| Window Glass | 9.8 - 13.8 | 64 |
| Schott Borosilicate Glass* | 16 | 39 |
| Alkali-silicate Glass | 200 | 3.1 |
| Glass-bonded Mica | 14.0 - 15.7 | 45 |
| Macor Glass Ceramic ** | 40 | 16 |
| Fused Silica | 470 - 670 | 1.3 |
| Alumina * | 13.4 | 47 |
| Alumina-silicate (Al_2SiO_5) | 5.9 | 106 |
| Boron Nitride | 37.4 | 17 |
| Zirconia PSZ *** | 9.8 | 63 |
| Porcelain | 35 - 160 | 18 |
| * Schott Borofloat glass: www.hextek.com | | |
| ** Macor: www accuratus.com | | |
| *** Insaco, Inc. Zirconia PSZ product data sheet | | |

4.0 CERAMIC/METAL SEALS

Ceramic/metal sealing was developed in the 1950s to improve sealing properties compared to glass/metal seals, including mechanical and dielectric properties, thermal shock resistance, and high temperature resistance [41]. Ceramic materials are inherently strong, but brittle. Their brittleness limits their usefulness in most applications. However, crystalline ceramic materials generally retain better mechanical properties at higher temperatures than metals. Ceramics generally provide better dielectric properties than glasses, as ceramics are usually good electrical insulators. Additionally, their relative chemical inertness makes ceramics suitable for many applications [42].

Ceramic/metal seals are commonly made with alumina (Al_2O_3) as the dielectric, and most of these seals are formed using the moly-manganese metallizing process combined with brazing [41]. Active brazing is another process commonly used for ceramic/metal bonding with both oxide and non-oxide ceramics, where the brazing filler metal contains reactive species that allow wetting of the braze metal to both the ceramic and metal surfaces. Brazing alloys include

refractory metal powders, precious metals, and active metals. For oxide ceramics, Ti-containing filler metals are widely used, which form TiO or Ti₂O₃ interfacial phases that promote wetting and bonding. Brazes can provide ductile strain relief for the interface between the metal and the ceramic through yielding and creeping, which reduces residual stresses (i.e. thermal stresses) [40]. Other ceramic/metal bonding techniques include diffusion (solid-state) bonding and fusion welding. Solid-state bonding can be performed with a large number of ceramic/metal systems, including Al₂O₃ on steel, Al, Ti, Cu, Ni, Pt, and Nb; SiO₂ on Al and Mg, ZrO₂ on Al and Mg, and MgO on Ni [43].

Both oxide and non-oxide ceramics should be considered for use as the feedthrough insulator. Common structural oxide ceramics include alumina (Al₂O₃), quartz silica (SiO₂), zirconia (ZrO₂), magnesia (MgO), beryllia (BeO), mullite (3Al₂O₃·2SiO₂), and various other silicate-based oxides and minerals (e.g. porcelain, feldspar, etc.). Non-oxide structural ceramics largely include nitrides, carbides, silicides, and borides. Braze alloys containing small amounts of reactive metals (e.g. Ti, Zr, or Al) can be used to promote wetting and reactions to join non-oxides to metals. The CTE of non-oxide ceramics is generally lower than that of the oxides; therefore ductile metal fillers are often used to prevent failure at the joint. Metallization layers can be formed from deposited reactive metal thin films. The active metal segregates to the interface and produces a thin transition layer, e.g. titanium nitride, carbide, and/or silicide. Solid-state bonding can also be used to join non-oxide ceramics to metals. The joint strength generally decreases as the thickness of the interlayer increases [44].

Eutectic joining can be performed for many ceramic/metal systems, where the metallic materials react with the ceramics to form eutectic liquids. For example, silicon nitride can be bonded to several different metals utilizing eutectic reactions. Thin reaction layers are often formed between the metal and ceramic (e.g. metal silicides). Room-temperature solid-state bonding of small parts can be performed at ultrahigh vacuum (i.e. around 10⁻¹⁰ torr). The metal to be bonded must be soft to deform under the pressure. One such system joined by this process is silicon nitride and aluminum. Reaction bonding of the interfaces can also be performed for certain systems, where the interlayer is converted to a joining material via reaction. Further details of the processing and design considerations for ceramic/metal seals are provided in Appendix A.

The ceramic component itself is formed by any of a variety of ceramic processing techniques. After sintering and densification of these ceramics from their powder form, grinding is performed to create the required dimensions. However, the grinding produces surface defects and potential failure sources. Therefore, resintering of the component is often performed to heal the grinding flaws.

Tailoring of the interlayer is often performed to obtain the paramount joint properties. This is especially true of non-oxide ceramics, which tend to have very low CTEs, creating a large CTE difference between the ceramic and the metal. Soft metal, composite (particulate and fibrous), and laminate (soft/hard metal) interlayers have been developed to enhance the properties of the joints.

4.1 MECHANICAL INTEGRITY OF CERAMIC/METAL SEALS

The mechanical integrity issues for ceramic/metal seals are generally the same as for glass/metal seals (see section 3.1). Table 5 presents physical and mechanical data for selected ceramic materials. These data can be compared to the glass, glass-ceramic, and metal alloy

data presented in Table 2 and Table 3. The strength and toughness of dense polycrystalline ceramics are generally greater than that of glasses. Thus, for mechanical durability, ceramic insulators would be preferred to glass insulators. However, because ceramic properties are much more difficult to tailor than those of glasses or glass-ceramics, the CTE mismatch between ceramic and metal will limit the potential ceramic/metal joint material combinations. CTE mismatch stresses may be reduced by utilizing a ductile braze alloy that could absorb some of the stress and strain. Thermal shock due to large temperature gradients across the ceramic may also be limiting. The electrical insulator chosen would ideally be highly thermally conductive in order to minimize the temperature gradient and the resulting thermal stresses. Because ceramics typically have very high compressive strength but low tensile strength, a reasonable level of residual compressive stress in the ceramic may be necessary to limit the effects of applied tensile stresses.

Table 5. Physical and mechanical properties of selected ceramics [19-34].

| Ceramics | Melting Point (K) | Density (g/cm ³) | Thermal Conductivity 300K (W/m·K) | Electrical Resistivity Ω·m (300K) |
|---|---|-------------------------------|-----------------------------------|--|
| Al ₂ O ₃ (99.9%) ^{d,e,r,q} | 2291 | 3.98 | 39.0 | >10 ¹³ |
| MgO ^{d,f,q,r} | 3125 | 3.6 | 38.0 | >10 ¹³ |
| Mullite ^{f,l,r} | - | - | 5.9 | - |
| BeO ^{i,d,s} | 2720 | 3 | 220 - 275 | - |
| Zirconia PSZ ^m | ~2125 | 5.8 | 1.8 - 3.0 | >10 ¹⁰ |
| Si ₃ N ₄ (reaction bonded) ^e | 2302 | 2.7 | 10.0 | >10 ¹² |
| Si ₃ N ₄ (hot pressed) ^e | 2302 | 3.3 | 29 | >10 ¹² |
| Porcelain ^{f,r} | - | - | 1.8 - 3.0 | >10 ¹² |
| SiC (hot pressed) ^e | 3012 | 3.3 | 80 | 10 ⁰ - 10 ⁹ |
| Graphite (extruded) ^e | - | 1.71 | 130 - 190 | (7-20)x10 ⁻⁶ |
| Ceramics | CTE α _{ave} × 10 ⁻⁶ 300K (K ⁻¹) | Elastic Modulus, E 300K (GPa) | Poisson's Ratio | Fracture Toughness (MPa·m ^{1/2}) |
| Al ₂ O ₃ (99.9%) ^{d,e,r,q} | 8.6 | 380 | 0.22 | 4.2 - 5.9 |
| MgO ^{d,f,q,r} | 13.5 | 210 | - | - |
| Mullite ^{f,l,r} | 5.3 | 145 | - | - |
| BeO ^{i,d,s} | 7.6 | 380 | - | - |
| Zirconia PSZ ^m | 10.1 | 200 | 0.23 - 0.31 | 7.0 - 12.0 |
| Si ₃ N ₄ (reaction bonded) ^e | 2.7 | 304 | 0.22 | 3.6 |
| Si ₃ N ₄ (hot pressed) ^e | 3.1 | 304 | 0.3 | 4.1 - 6.0 |
| Porcelain ^{f,r} | 6.0 | ~70 | - | - |
| SiC (hot pressed) ^e | 4.6 | 207 - 483 | 0.17 | 4.8 - 6.1 |
| Graphite (extruded) ^e | 2.0 - 2.7 | 11 | - | - |

* References are the same as in Table 2.

The failure of ceramic joints arises from source defects at the interface or in the bulk of the material. Cracks may originate at these defects due to external and/or residual stresses, which are exacerbated by stress concentrations, especially in the region of the joint. The defects may be created during formation (i.e. sintering) processes, or they may be a result of other fabrication processes such as machining, which often induces significant defects at or just below the ceramic surface. Chemical reactions at the interface can produce other defects such as gaseous voids [43]. The defects must be limited to produce a robust ceramic/metal seal.

4.2 CHEMICAL INTEGRITY OF CERAMIC/METAL SEALS

The chemical reactivity of most crystalline ceramics is generally lower than that of glasses. While most of the same glass/metal joint chemical integrity concepts also apply to crystalline ceramic/metal joints (see section 3.2), the reactivity and diffusivity of chemical species are generally lower in dense ceramic materials than in glasses. The enhanced chemical integrity provided by some ceramics may be required for this feedthrough application. Diffusivity of helium through dense ceramics is low, and is not expected to be an issue as long as the ceramic does not develop cracks and/or significant levels of porosity.

4.3 ELECTRICAL INTEGRITY OF CERAMIC/METAL SEALS

Electrical integrity of ceramic/metal seals is generally similar to that for glass/metal seals, as presented in section 3.3. The dielectric breakdown strength of ceramics is similar to that of glasses, as shown previously in Table 4. Crystalline ceramic materials are often better electrical insulators than glasses, and therefore might be preferred on the basis of their greater resistivity.

5.0 POLYMER/METAL SEALS

Polymer/metal seals are frequently used in hermetic electrical feedthrough pressure and vacuum applications. The thermal and radiation resistance of polymers is limited, and it was determined that polymer-based seals would be avoided for this application. However, polymers could still find potential use in this or other similar applications if (a) the specifications changed with lower maximum temperature and lower neutron radiation levels, or if (b) new polymers were developed with higher temperature and radiation resistance. For example, a higher-temperature polyimide-based polymer called Celazole PBI, with a maximum service temperature of 600 K (620°F), has been developed recently [45].

Polymer/metal electrical feedthroughs are based primarily on mechanical seals. A polymer gland is placed into a feedthrough assembly, which butts up against both the conducting wire and the body (see Figure 5.h and i). Liquid sealants may be applied to the gland surface to assist in wetting the metal. Utilizing axial compression, the polymer gland deforms axially and expands radially, producing a tight hermetic seal. More details about this type of feedthrough can be found in References 3 and 9. These feedthroughs are especially useful for low-temperature, low-stress applications.

6.0 PROPOSED TESTING

Initial testing for the electrical feedthroughs was to be designed and performed by the SE activity at Bettis (see Reference 46). These tests included initial in-house testing of vendor-supplied feedthroughs. First, a vibratory test would be performed that would simulate a launch. Preliminary helium leak testing would also be performed using a "gas sniffer wand." If the feedthroughs passed these tests, they would be sent to NASA Glenn Research Center for the next phase of testing. This second phase would include thermal cycling tests between 100°F (310 K) and 500°F (535 K) at 2000 kPa pressure, with He leakage rates monitored by a mass spectrometer [46].

6.1 INITIAL HELIUM LEAK TESTING

Additionally, more specific materials-based testing was proposed by the Bettis MT-AMSI group. This testing included more basic, component-specific testing to better characterize the individual material components of the feedthroughs. The salient data concerning the hermeticity of glass/metal and ceramic/metal seals is helium leakage. As discussed earlier, helium diffusion through glass and ceramics is much greater than xenon diffusion, making helium permeation the limiting factor in system hermeticity. In addition, xenon is quite costly and may be impractical to use in leak tests. General guidelines concerning gas leakage are found in ASTM E 479-91, "Standard Guide for Preparation of a Leak Testing Specification" [47]. For the current application, leakage could be measured using a mass spectrometer to detect and quantify helium leakage rates as low as 10^{-9} standard cc/sec. Mass spectrometer helium leak tests are described in both ASTM designations E 493-97, "Standard Test Methods for Leaks Using the Mass Spectrometer Leak Detector in the Inside-Out Testing Mode," [48] and E 1603-99, "Standard Test Methods for Leakage Measurement Using the Mass Spectrometer Leak Detector or Residual Gas Analyzer in the Hood Mode" [49]. ASTM E 493 is intended for testing semiconductors, hermetically enclosed relays, pyrotechnic devices, etc., while E 1603 is intended for larger scale components, such as the feedthrough application described herein. Both methods use the same principles: fill the component with helium, create a vacuum around the component, and then measure the helium leakage rate using a mass spectrometer. A basic schematic of method E 1603 is shown in Figure 8. In this test, a continuous supply of helium gas is provided to the component. The ASTM standard recommends that the helium leakage measurements be made by a qualified technician according to NDT standards. Further details on leak testing can be found in Reference 50.

A modified procedure roughly following E 1603 might be the optimal method of testing hermeticity in Brayton feedthroughs. Figure 9 shows a schematic of this proposed test. First a seal, which could be seamlessly attached to tubing on both sides, would be made around a wire. One side of the seal would be connected to a gas regulator attached to a helium cylinder. The regulator would be used to maintain a constant helium pressure of 4000 kPa on one side of the seal. The other side of the seal would be attached to a vacuum system and a leak detector (i.e. mass spectrometer). The vacuum system should be able to create a vacuum of at least 10^{-6} torr and would consist of a mechanical pump in combination with an oil diffusion pump, or a turbo pump alone. This vacuum is considerably less than the vacuum of space, $\sim 10^{-14}$ torr, but would provide a practical means for initial testing of feedthroughs. The feedthrough assembly would then be placed in a tube furnace or surrounded by heating coils in order to measure helium leakage at the service temperature of 500-550 K (440-530°F). Additionally, thermal cycling could be performed with simultaneous real-time leak testing. A tube capable of transporting liquid nitrogen, 77 K (-320°F), could also be coiled around the seal in order to cool

the feedthrough to the minimum anticipated temperature of 200 K (-100°F). Multiple thermocouples should be placed on the seal to accurately control the temperature of the feedthrough. An alternative feedthrough helium leak testing design very similar to this was proposed in Reference 46.

An initial leak testing plan for the Prometheus feedthroughs should also include endurance testing of the seals at temperature and pressure, thermal cycling, and vibration loads that simulate the conditions expected at ground launch. These tests should be performed prior to or during helium leak testing of the feedthroughs to verify that the feedthroughs are capable of withstanding the conditions imposed prior to reactor startup. A test design similar to this is proposed in Reference 46.

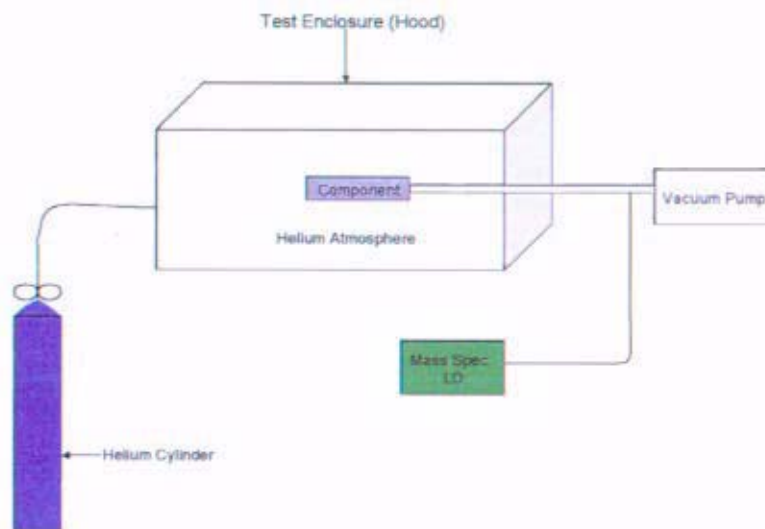


Figure 8. Schematic of ASTM E 1603: helium leak testing using mass spectroscopy.

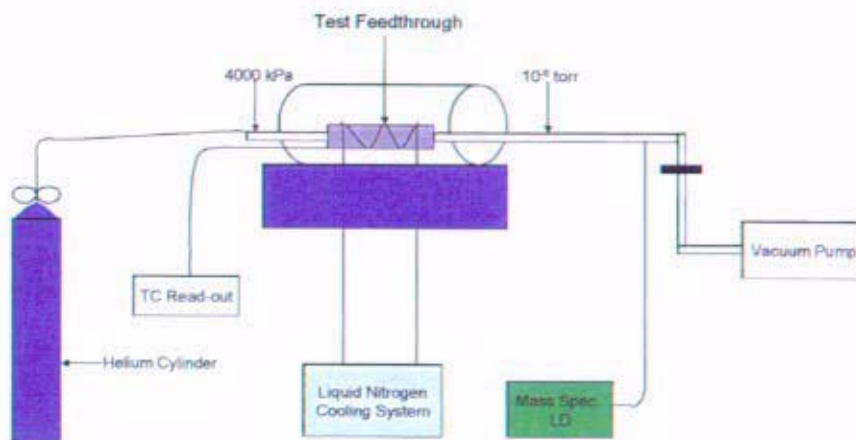


Figure 9. Schematic of proposed helium leak testing rig.

6.2 INITIAL MECHANICAL AND ELECTRICAL PROPERTY TESTING

There are many properties of the electrical feedthrough, specifically properties of the insulator material and the insulator/conductor joint, that should be measured to determine a suitable insulator material. These include mechanical property and electrical property measurements at various extreme conditions expected in the Prometheus application.

Mechanically, the joint and specimen strength and durability are important to this application. Ideally, all cracking of the ceramics and glasses would be avoided to prevent coolant leakage paths, component fracture, and other harmful effects. Axial cracks in the insulator (along the length of the wire) that produce delamination of the seals would especially be critical, but radial cracks in the insulator (perpendicular to the wire) should also be avoided to maintain component integrity. Additionally, radial cracks within the insulator may produce electrical shorts, especially if any metal migration occurs along the surface of the crack. Moreover, if the conducting wire(s) became embrittled during service, i.e. by radiation exposure, temperature exposure, mechanical work, and/or chemical diffusion, radial cracks formed in the insulator could propagate through and fracture the entire component, severing the electrical connection between the alternator and the rest of the spacecraft electrical system. Thermal expansion mismatch stresses at the interfaces could be significant, depending upon the design of the component. It is expected that the feedthrough components would not be subjected to other large applied external stresses, however it should be verified that the components have significant mechanical integrity. Cylindrical specimens of wire/insulator/body materials should be bend-tested for strength and toughness of both the joint and the full component. Standard four-point bend testing of the feedthrough assemblies should be performed after various stages of vibration, irradiation, thermal cycling, and other conditions that might be expected during the mission. Three-point bending can also be performed to more directly test the joint strength. The chemical strength and toughness of the interfaces may also be tested using single-edge-notched beam bend testing or double-cantilever beam testing. All of these procedures are briefly described in Reference 43.

In terms of initial electrical testing, the feedthrough must insulate the conducting wire from the body, which connects to the coolant piping system. Electrical failure of the insulator will short circuit the system. As shown in Table 4, a very thin layer of insulating material is required to electrically insulate the conductor without dielectric breakdown. However, as the exact conditions in the system, including spikes in voltage and/or current, are unknown, a large safety factor would have to be made in terms of insulator thickness in order to verify system electrical integrity. Initial electrical testing of the feedthrough component would serve two main purposes: (i) the electrical properties (specifically the dielectric breakdown strength) of the insulator could be tested after exposure to the conditions of the system, i.e. thermal cycling, mechanical stress cycling, exposure to coolant gas and vacuum environments, and irradiation; and (ii) by finding the dielectric breakdown voltage of the component and applying statistics, an appropriate safety factor could be obtained for production of the final feedthrough.

7.0 POTENTIAL VENDORS

Hamilton Sundstrand was identified as a potential vendor for the turboalternator. For the alternator electrical feedthroughs, several potential vendors were identified, as introduced below. This initial list is by no means complete.

CeramTec North America Corporation (Laurens, SC) is the "world leader in ceramic-to-metal sealing technology." Through their Ceramaseal[®] product lines, CeramTec produces ceramic/metal hermetically-sealed feedthroughs for ultra-high vacuum or high-pressure environments over a wide range of temperatures (see Figure 5 a-c for examples). Ceramaseal[®] product applications have included high pressure, high temperature, high voltage, nuclear, aerospace, and sensor applications. Most of the CeramTec hermetic ceramic-to-metal seals are metallized hard-bonded and brazed seals with high-purity alumina as the insulator. Metals bonded with alumina include a wide variety of alloys, including Kovar[®], stainless steel, nickel, copper, nickel-iron alloys, cupro-nickel alloys, molybdenum, Alumel[®] and Constantan[®], with braze metals silver, copper, and gold alloys. The dielectric strength of the high-purity alumina insulator is about 31.5 kV/mm (800 V/mil) [5]. The majority of their products are guaranteed for use up to 725 K (840°F), and actual usage temperatures can often exceed 725 K [51]. Additionally, CeramTec hermetic seals can be designed for use under ultra-high vacuum conditions and/or under high pressure conditions (in excess of 25,000 psi, or 170 MPa). Each Ceramaseal[®] product is guaranteed hermetic to 10^{-9} atm cc/sec He and is rated for currents over 1000 A and voltages over 100 kV. All of these conditions individually met or exceeded the Prometheus alternator general requirements. However, representatives at CeramTec did not give a definitive answer to whether or not they could produce a hermetic seal that encompassed all of the specific design requirements.

Hermetic Seal Corporation (HSC) (HCC Industries, Rosemead, CA) specializes in glass/metal seals [52]. HSC promotes chromium, iron, nickel, and Inconel as metals that produce good oxide coatings applicable to glass wetting. Copper, molybdenum and titanium do not produce appropriate oxide coatings, and may require an outer sheath to induce wetting of the glass. The HSC glasses of preference included borosilicates (5-20% boron oxide [53], low coefficient of thermal expansion) and Ba-alkali borosilicates. The thermal compression mismatch of the insulator and conductor is utilized such that the glass/metal compression fit alone produces a seal with a helium leak rate of 10^{-7} std cc/sec. Through fusion bonding of the glass to the conductor, leak rates can be reduced to a best-case scenario of 10^{-11} std cc He/sec. The leakage rates increase with increased temperature and pressure. HSC specializes in glass-to-Inconel seals, including proprietary glass L21 bonded to Inconel X-750. Other alloys employed by HSC include stainless steel, Kovar[®], Monel, 52 alloy, Hastelloy, Alumel[®], Chromel[®], and Constantan[®]. HSC seals have withstood 20 year flight times in aircraft. HSC had sent some of their glass samples to Bechtel Bettis, Inc. for testing, but these samples were recalled upon notice of termination of the space reactors program.

Alberox Products (Morgan Advanced Ceramics, New Bedford, MA) produces custom ceramic/metal seals and assemblies. Alberox claims benefits for their seals compared to glass/metal seals in terms of stability at high temperatures, electrical properties, durability, and strength. Alberox is primarily a custom part manufacturer. Their primary insulator material is a 95% alumina ceramic (A950). They also work with higher purity alumina, sapphire, ruby, aluminum nitride, zirconia, silicon carbide, and silicon nitride. Typical metals for bonding include nickel, Inconel, Ni-Fe, Ni-Fe-Co (Kovar[®]), refractory metal, copper, platinum, titanium, and stainless steel alloys. A metallizing process is used to prepare the ceramics, and the joints are

brazed. Typical braze alloys include copper, gold, silver, and nickel alloys. Alberox claims hermetic seals to better than 10^{-9} cc/sec He [54].

Conax Buffalo Technologies (Buffalo, NY) specializes in mechanical insulator/conductor seals (see Figure 5 h-i for examples). The seals are made by the axial compression of a compressible gland such that radial compressive stresses at the sealant/wire and sealant/body interfaces hermetically seal the component. Conax specializes in polymer and plastic sealants (or glands); however they also have experience with crushable ceramic particles and dense boron nitride insulators. The polymer-insulated components hermetically seal the components, but the ceramic components are known to have gas leakage issues [55]. The Conax polymers most useful at high temperatures are Viton[®] and Teflon[®] fluoropolymers (maximum usage temperature 507 K) and Vespel[®] polyimide (533 K). The maximum temperature stabilities and radiation tolerances of Viton[®] and Teflon[®] are dubious with respect to the design requirements. Although the general properties of Vespel[®] appear satisfactory, concerns remain about the thermal resistance, radiation resistance, low-stress plastic deformation and outgassing properties of these polymers. Thus, more robust materials such as glasses and ceramics were pursued instead. One such choice still remained with respect to Conax. A hermetically sealing material that Conax uses for optical fiber feedthroughs is Grafoil[®] (compressible foil layers of graphite). Since Grafoil[®] is electrically conductive, it could not serve as the electrical insulator by itself. However, the author proposed that a ceramic electrical insulator could be hermetically sealed to the conductor and the feedthrough body by supplying compressible Grafoil[®] at both the insulator/wire and insulator/casing interfaces; and then subjecting the entire feedthrough to significant radial compression. In this manner, mechanical hermetic seals should form between the wire and the Grafoil[®], and between the Grafoil[®] and the body. The possibility also seemed to exist that the Conax-type fitting might work with a ceramic insulator brazed to both the body and the wire.

Schott North America, Inc., Electronic Packaging Division (Southbridge, MA) produces glass/metal seals for many applications, including large-scale electrical feedthroughs. Their glass/metal seals utilize conducting wires enclosed by preformed sintered glass packages, which are enclosed by external metal parts. Schott utilizes both matched and compression seal designs. Schott has a line of proprietary glasses for use in different conditions, including both hard and soft glasses. The glasses are often sealed with Ni-Fe, Ni-Co, or Cr-Ni alloys, or various steels and other alloys. Schott glass/metal seals are applicable up to 525 K (480°F), and certain material combinations can be made to withstand temperatures up to 725 K (840°F). A typical dielectric breakdown strength for Schott glass is about 20 kV/mm (500 V/mil) [56].

Tekna Seal, LLC (Minneapolis, MN) produces hermetic ceramic/metal and glass/metal seals. Insulator materials include borosilicate, Ba-alkali, soda-lime, and low silica glasses; glass-ceramics; and zirconia and alumina ceramics. Conductor materials include Ni-Fe, stainless steel, Kovar[®], and copper alloys. Their components can be used up to 475 K (390°F), and up to 875 K (1110°F) with glass-ceramics. Some of their seals are capable of withstanding pressures over 20 ksi (140 MPa). Helium leakage rates of their seals are listed as less than 10^{-10} atm cc/sec. Tekna Seal utilizes both matched and compression-type seals. In particular, their matched seals are most often made with Kovar[®] pins and housings (wires and bodies) with borosilicate glass insulation. Their glass-ceramic insulators may be used with conductors such as stainless steel, superalloys, nickel, copper, Alumel[®], and Chromel[®] alloys. Tekna Seal claims helium hermeticity to 10^{-10} std cc/sec through their glass seals [57].

MDC Vacuum Products Corp. (Hayward, CA) produces a wide variety of electrical feedthroughs utilizing ceramic/metal seals. Various materials are used in their feedthroughs, which are

applicable to ultrahigh vacuum levels, high voltages and currents, and elevated temperatures up to about 725 K (840°F). MDC produces single and multiple wire feedthroughs for a multitude of applications [7].

Latronics Corporation (Latrobe, PA) produces hermetic ceramic/metal and glass/metal made-to-order seal assemblies for both low and high-volume requirements. Latronics produces custom feedthroughs specific to the electrical, temperature, and environmental conditions required. They also produce some standard parts. For glass/metal seals Latronics offers a product line and features matched expansion seals using Kovar®. Compression and specialty combination seals are also produced. All seals are tested to at least 10^{-8} cc/sec helium hermeticity [6].

Solid Sealing Technology, Inc. (SST) (Watervliet, NY) produces hermetic vacuum feedthroughs among a wide range of ceramic/metal and glass-ceramic/metal seals. Specifications include temperatures up to 725 K (840°F), pressures ranging from high pressure to ultra-high vacuum, voltages over 200 kV, and currents greater than 1000 A. Ceramic/metal seals are produced through thickfilm metallization (molybdenum) of alumina ceramics. Brazing is then performed with metals including high nickel, copper, and precious metal alloys. SST also utilizes one-step active metal brazing (Ti or Zr active metals) of ceramics to metal. Active metal brazing is suited for sealing sapphire, larger ceramics, and non-oxide ceramics. Glass-ceramic sealing is performed by SST utilizing high temperature (up to 675 K), high thermal expansion glass-ceramic materials. Glass-ceramic sealing is used to seal 304 and 316 stainless steels for high vacuum/high pressure applications [8].

Comus International (Clifton, NJ) produces hermetic glass/metal seal assemblies and feedthroughs. Comus produces compression seals utilizing Ba-alkali, Pb-silicate, and soda-lime glasses sealed to bodies of Inconel or stainless steel, and electrodes of Fe-Ni alloys 52 or 42. Comus compression seals withstand temperatures up to 725 K (840°F). Comus also produces matched seals utilizing borosilicate (alkali, barium, soda, and potash) glasses sealed to Kovar®, tungsten, or molybdenum. Comus does not recommend their matched seals for use above 525 K (480°F). Combinations of other materials can also be made. Comus guarantees helium hermeticity to 10^{-8} std cc/sec, but their seal hermeticity typically tests between 10^{-9} and 10^{-10} std cc/sec [58].

Other companies of interest include, but are not limited to: IJ Research, Inc. (Santa Ana, CA), which produces hermetic ceramic/metal and glass/metal seals [59]; Accratronics Seals Corp. (Burbank, CA), which produces hermetic ceramic/metal and glass/metal seals (300 series stainless steel, Kovar®, Inconel, Rodar®, steel, or Fe-Ni 52 alloy) [60]; Hermetic Seal Technology, Inc. (Cincinnati, OH), which produces glass-to-metal hermetic seals [61]; and Dash Connector Technology (Spokane, WA), which manufactures standard or custom hermetically sealed electrical connectors [62].

8.0 SUMMARY AND CONCLUSIONS

Helium leakage through the electrical feedthroughs for the Brayton cycle space nuclear power plant was determined to be a critical issue to the success of the Prometheus mission. Preliminary spacecraft and power plant designs led to specifications for the feedthroughs, which were in the process of being researched by personnel in the MT and SE activities at Bechtel Bettis, Inc. when the program was terminated. After initial consideration of the available materials, it was determined that temperature and radiation conditions limited the insulator materials to ceramics and glasses. Properties of ceramics, glasses, and glass-ceramics, along with the properties of conducting alloys were presented and discussed in terms of mechanical, chemical, and electrical integrity. A set of initial testing procedures was proposed, including helium leak testing and preliminary mechanical and electrical property testing. Potential vendors in the areas of ceramic/metal, glass/metal, and polymer gland mechanical compression seals were identified.

From initial considerations, ceramic/metal seals looked the most promising for the Prometheus application because of their superior thermal, mechanical, chemical, and radiation integrity. However, the easier processing of glass/metal seals and the ability to better tailor the thermal expansion properties of glass/metal and glass-ceramic/metal joints showed that glass-based insulators should also be considered for initial work. It is likely that one or more of several potential vendors would have been able to produce electrical feedthroughs that could work for this application. Had the Prometheus program continued, it would have been recommended that a number of commercial feedthroughs be procured, including a variety of ceramic, glass, and glass-ceramic insulated feedthroughs; and then tested following protocol similar to that presented herein. The limitation from the initial specifications would have been that the insulator is compatible with and hermetically sealed to an Inconel or other superalloy feedthrough body, since the body of the feedthrough must be compatible with the Inconel 617 or 625 coolant piping system. From the study of some of the commercial vendors, ceramic/Inconel (i.e. alumina/Inconel) and glass/Inconel seals are currently in production. It is recommended that the conductor and insulator material choices for initial testing be made in consultation with experienced vendors.

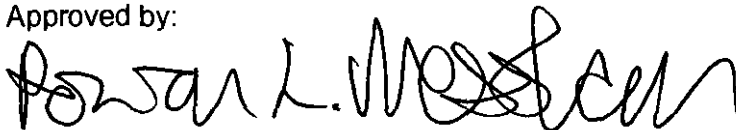


Jason K. Clobes, Senior Engineer
Advanced Materials System Integration
Materials Technology



Andrew M. Ruminski, Engineer
Advanced Materials System Integration
Materials Technology

Approved by:



R. L. Messham, Manager
Advanced Materials System Integration
Materials Technology

REFERENCES

1. Bechtel Bettis, Inc., B-SE(SPS)-001, Prometheus project report SPP-67110 section 9 "Component Descriptions," Bechtel Bettis, Inc., 2006.
2. NGST Report 04.1F102.JM.006, "Task 2 Conceptual Design Summary Report, Jupiter Icy Moons Orbiter (JIMO) Phase A Study, JPL Contract N. 120530," Aug. 13, 2004.
3. D'Antonio, John, B-SE(SPS)-001, Prometheus project report SPP-67110 sections §9.1.5 "Alternator Description," and §9.1.8 "Failure Modes," Bechtel Bettis, Inc., 2006.
4. Pheil, Edward and Audra Rice, KAPL, phone conversation, Aug. 2005.
5. CeramTec North America Corporation, company website, <http://www.ceramaseal.com>, viewed Sep. 2005.
6. Latronics Corporation, company website, <http://www.latronicscorp.com>, viewed Nov. 2005.
7. MDC Vacuum Products Corp., company website, <http://www.mdcvacuum.com>, viewed Nov. 2005.
8. Solid Sealing Technology, Inc., company website, <http://www.solidsealing.com>, viewed Nov. 2005.
9. Conax Buffalo Technologies, company website, <http://www.conaxbuffalo.com>, viewed Nov. 2005.
10. Richardson, Chris, "Wire Sizing for the Connector of the Brayton Alternator," KAPL, unpublished, 2005.
11. Gribik, Anastasia, "Gas Leakage White Paper," Bechtel Bettis, Inc., Feb. 28, 2005.
12. D'Antonio, John, "Gas Leakage and Electrical Passthrough Overview," Bechtel Bettis, Inc., Space Engineering (SE) Activity, Space Fluid and Mechanical Systems Design, presented Aug. 5, 2005.
13. Clobes, Jason, "Materials Properties of Concern in Brayton Alternator Power Feedthrough Potting Dielectric," Bechtel Bettis, Inc., unpublished, Aug. 16, 2005.
14. Tomsia, A. P., J. A. Pask, and R. E. Loehman, "Glass/Metal and Glass-Ceramic/Metal Seals," in *Engineered Materials Handbook Volume 4: Ceramics and Glasses*, ASM International, pp. 493-501, 1991.
15. Kingery, W. D., H. K. Bowen, and D. R. Uhlmann, *Introduction to Ceramics*, Second Ed., John Wiley & Sons, pp. 91-124, 1976.
16. Watkins, R. D., "Types of Ceramic Joining and Their Uses," in *Engineered Materials Handbook Volume 4: Ceramics and Glasses*, ASM International, pp. 478-481, 1991.
17. Loehman, R. E., and A. P. Tomsia, "Joining of Ceramics," *Ceramic Bulletin*, vol. 67 [2], 375-380, 1988.
18. Borom, M. P., A. M. Turkalo, and R. H. Doremus, "Strength and Microstructure in Lithium Disilicate Glass-Ceramics," *Journal of the American Ceramic Society*, vol. 58 [9-10], 385-391, 1975.

19. Everhart, J. L., *Engineering Properties of Nickel and Nickel Alloys*, Plenum Press, pp. 8-31 and 58-81, 1971.
20. "Metallurgy, Processing, and Properties of Superalloys," *ASM Specialty Handbook: Heat-Resistant Materials*, ed. J. R. Davis, ASM International, pp. 221-254, 1997.
21. Mankins, W. L., and S. Lamb, "Nickel and Nickel Alloys," *ASM Handbook Volume 2: Properties and Selection: Nonferrous Alloys and Special-Purpose Materials*, ASM International, pp. 428-445, 1990.
22. Robie, R. R., B. S. Hemingway, and J. R. Fisher, *Thermodynamic Properties of Minerals and Related Substances at 298.15 K and 1 Bar (10⁵ Pascals) Pressure and at Higher Temperatures*, U.S. Geological Survey Bulletin 1452, 1979.
23. Callister, W. D. Jr., *Materials Science and Engineering: An Introduction*, Sixth Edition, John Wiley & Sons, Inc., pp. 737-770, 2003.
24. *Kirk-Othmer Encyclopedia of Chemical Technology*, Third Edition, Volumes 5 and 11, John Wiley & Sons, 1979.
25. "Properties of Pure Metals," *ASM Handbook Volume 2 – Properties and Selection: Nonferrous Alloys and Special-Purpose Materials*, ASM International, pp. 1099-1198, 1990.
26. Schott Technical Glasses Physical and Technical Properties, corporate literature, Dec. 2002.
27. High Temp Metals, Kovar[®] product technical data sheet, www.hightempmetals.com/techdata/hitempKovardata.php, viewed Nov. 2005.
28. Morey, G. W., *The Properties of Glass*, Second Edition, Reinhold Publishing Corporation, p. 276, 1954.
29. Insaco, Inc., Zirconia PSZ product data sheet, www.insaco.com/MatPages/zirconia-psz.asp, viewed Nov. 2005.
30. H. Cross Company, Alloy 42 and 52 product data sheet, www.hcrosscompany.com/metals/alloy4252.htm, viewed Dec. 2005.
31. Special Metals, NILO[®] and NILOMAG[®] Nickel-Iron Alloys product data sheet, www.specialmetals.com, viewed Dec. 2005.
32. Goodfellow Alumel[®], Chromel[®], and Constantan[®] product data sheets, www.goodfellow.com, viewed Dec. 2005.
33. *CRC Handbook of Chemistry and Physics*, 83rd Edition, ed. D. R. Lide, CRC Press, 2002.
34. Cengel, Y., and R. Turner, *Fundamentals of Thermal-Fluid Sciences*, McGraw-Hill, 2001.
35. Shelby, J. E., W. C. Lacourse, and A. G. Clare, "Engineering Properties of Oxide Glasses and Other Inorganic Glasses," in *Engineered Materials Handbook Volume 4: Ceramics and Glasses*, ASM International, pp. 845-857, 1991.
36. Partridge, J. H., *Glass-to-Metal Seals*, p. 216, The Society of Glass Technology, 1949.
37. Jost, W., *Diffusion in Solids, Liquids, and Gases*, Academic Press Inc., Publishers, pp. 287-288, 300, 1952.

38. Shelby, J. E., "Effect of Phase Separation on Helium Migration in Sodium Silicate Glasses," *Journal of the American Ceramic Society*, Vol. 56 [5], 263-266, 1973.
39. Zinkle, Steve, "Overview of Radiation Effects in Polymers, Semiconductors, and Ceramic Insulators," Oak Ridge National Laboratory, presented Nov. 10, 2004.
40. Beauchamp, E. K., and S. N. Burchett, "Techniques of Seal Design," in *Engineered Materials Handbook Volume 4: Ceramics and Glasses*, ASM International, pp. 532-541, 1991.
41. Mizuhara, H., and T. Oyama, "Ceramic/Metal Seals," in *Engineered Materials Handbook Volume 4: Ceramics and Glasses*, ASM International, pp. 502-510, 1991.
42. M. M. Schwartz, *Ceramic Joining*, ASM International, 1991.
43. Moorhead, A. J., and H.-E. Kim, "Joining Oxide Ceramics," in *Engineered Materials Handbook Volume 4: Ceramics and Glasses*, ASM International, pp. 511-522, 1991.
44. Suganuma, K., "Joining Non-Oxide Ceramics," in *Engineered Materials Handbook Volume 4: Ceramics and Glasses*, ASM International, pp. 523-531, 1991.
45. Murari, A., and A. Barzon, "Ultra High Vacuum Properties of Some Engineering Polymers," *IEEE Transactions on Dielectrics and Electrical Insulation*, vol. 11 [4], 613-619, Aug. 2004.
46. Hunnell, Charles, B-SE(SPS)-001, Prometheus project report SPP-67110 section 17.4.2.3 "Gas Leakage Test", Bechtel Bettis, Inc., 2006.
47. ASTM Designation E 479-91, "Standard Guide for Preparation of a Leak Testing Specification," ASTM International, 2000.
48. ASTM Designation E 493-97, "Standard Test Methods for Leaks Using the Mass Spectrometer Leak Detector in the Inside-Out Testing Mode," ASTM International, 1997.
49. ASTM Designation E 1603-99, "Standard Test Methods for Leakage Measurement Using the Mass Spectrometer Leak Detector or Residual Gas Analyzer in the Hood Mode," ASTM International, 1999.
50. *Nondestructive Testing Handbook: Leak Testing*, 3rd Edition, ed. Patrick Moore, American Society for Nondestructive Testing Inc., 1998.
51. Renoski, Kevin, CeramTec North America Corp., Hermetic Seals Div., phone conversation, Sept. 2005.
52. Hermetic Seal Corporation, teleconference meeting, Aug. 2005.
53. Henkel, D., and A. Pense, *Structure and Properties of Engineering Materials*, Fifth Edition, McGraw-Hill, pp. 416-423, 2002.
54. Morgan Advanced Ceramics, company website, <http://www.alberox.com>, viewed Sept. 2005.
55. Crawford, Bob, Conax Buffalo Technologies, phone conversation, Aug. 2005.
56. Schott North America, company website, <http://www.us.schott.com>, viewed Dec. 2005.
57. Tekna Seal, LLC, company website, <http://www.teknaseal.com>, viewed Dec. 2005.
58. Comus International, company website, <http://www.assemtech.co.uk/glass.asp>, viewed Dec. 2005.

59. IJ Research, Inc., company website, <http://www.ijresearch.com/index.php>, viewed Dec. 2005.
60. Accratronics Seals Corp., company website, <http://www.accratronics.com>, viewed Dec. 2005.
61. Hermetic Seal Technology, Inc., company website, <http://www.glass-to-metal.com>, viewed Dec. 2005.
62. Dash Connector Technology, company website, <http://www.dashconnector.com/maininfo.htm>, viewed Dec. 2005
63. Green, D. J., *An Introduction to the Mechanical Properties of Ceramics*, Cambridge University Press, pp. 210-231, 1998.
64. Chambers, R. S., F. P. Gerstle, and S. L. Monroe, "Viscoelastic Effects in a Phosphate Glass-Metal Seal," *Journal of the American Ceramic Society*, vol. 72 [6], 929-932, 1989.
65. Pask, J. A., and A. P. Tomsia, "Wetting, Surface Energies, Adhesion, and Interface Reaction Thermodynamics," in *Engineered Materials Handbook Volume 4: Ceramics and Glasses*, ASM International, pp. 482-492, 1991.
66. Hokanson, H. A., S. L. Rogers, and W. I. Kern, "Electron Beam Welding of Alumina," *Ceramic Industry*, vol. 81 [2], 44-47, 1963.

APPENDIX A: CONCEPTS IN THE JOINING OF METALS TO RIGID MATERIALS

This page intentionally blank

A.1 Introduction

There are many issues associated with the creation of robust, hermetic bonds of glasses and ceramics to metal conductors, many of which are connected to the design of the component and with the bonding process conditions. There are three main requirements behind the formation of successful chemically-bonded material joints: (i) intimate contact between the materials, (ii) a strong chemical bond between materials, and (iii) the accommodation of thermal expansion mismatch stresses during fabrication and during operation. Minimal stresses at the interfaces and favorable stress gradients in the interfacial zones are desired to produce strong seals [42].

Metal seals with rigid materials are generally divided into three types: glass/metal, glass-ceramic/metal, and ceramic/metal seals. Of these, glass/metal seals are the most common, but glass-ceramic and ceramic insulators often have property advantages over glass insulators. Hermetic glass/metal seals have been used in electronics applications for several decades. Glass/metal seals are easy to manufacture, relatively inexpensive, and are generally reliable under moderate thermal and mechanical loads [16]. However, the suitability of glass/metal seals for specific applications is limited by temperature and strength. Such seals are usually produced by fusion bonding, where molten glass is applied to and reacts with the surface of the metal to produce strong chemical bonds upon cooling.

The incorporation of microcrystalline ceramic particles into the glass matrix, termed glass-ceramics, can enhance specific properties of the insulator. For example, glass-ceramics can provide increased strength and toughness to the insulator compared to typical glasses. Glass-ceramics can also be tailored to produce more compatible thermal expansion characteristics with metal substrates than typical glasses and ceramics. Glass-ceramics provide relative ease of processing, compared to ceramics, by utilizing molten glass wetting and bonding. Subsequent nucleation and crystallization of the ceramic reinforcing phases, however, requires carefully controlled heat-treatment processes. Glass-ceramic seals find use in nuclear feed-through seals where mechanical integrity at high temperatures and pressures is required [16].

Ceramic/metal seals (specifically, crystalline ceramics) have many potential advantages over glass/metal seals. They are typically stronger and less flaw-sensitive (higher toughness). Furthermore, they tend to be more resistant to high temperatures, less sensitive to thermal shock, and better dielectrics than glasses. These property enhancements can lead to longer life and higher vacuum capability than for similar glass/metal components [41]. However, the processing of ceramic/metal seals is much more complex than that for glass/metal seals. Ceramic/metal joining is usually accomplished through brazing, which is often performed with ceramics that have metallized surfaces. Metallized surfaces improve the wetting and adherence of the braze alloy to the ceramic. Ceramics can also be bonded to metals using molten glasses, provided the subsequent tensile forces near the interface are minimized [16]. However, brazing with glasses is usually limited to the joining of ceramics to ceramics.

The achievement of hermeticity depends on the design of a seal and its mechanical, chemical, and electrical characteristics. Mechanical reliability of a seal depends to a large extent on the CTE difference between the bonded materials and the residual and applied stresses at the interfaces and within the joined materials. To obtain strong chemical bonding at an interface, sufficient surface wetting between adjacent materials usually is required along with appropriate

interfacial reactions. An intermediate phase at the interface and special surface preparation techniques are often required for these reactions to occur. Braze alloys are usually used to create strong bonds; however solid-state bonding processes can also be used. Each of these concepts is elaborated upon in the following sections.

A.2 Seal Design

Design of the seal is important to its performance. The production of strong, reliable, and hermetic seals depends on the chemical and physical characteristics of the bonding. The microstructure of the materials around the interface and the reactions between the materials at the interface dominate the chemical properties of the seal. Residual and applied stresses, particularly significant tensile stresses in the brittle insulating component, must be avoided. CTE mismatch is often a source of large residual stresses. Near-match of material thermal expansion coefficients over the temperature range of processing/use is usually desired to avoid the creation of large thermal stresses. Figure A.1 presents examples of the degree of thermal expansion expected for a number of alloys (along with an alumina ceramic) over a large range of temperatures (the CTE values are the derivatives of the curves in these graphs). A closer CTE match is more important for larger ceramic and glass specimens than for thin coatings.

Matched compression seals or reinforced compression seals are often used to prevent tensile failure of a ceramic or glass insulator. For the standard matched compression seals, the internal wire and the insulator materials have closely matched thermal expansion coefficients while the external body (housing) has a considerably higher CTE. In this manner, compressive stresses are induced within the feedthrough materials by the outer body upon cooling from higher temperature. For reinforced compression seals, the CTE of the wire, or "pin," is also lower than that of the insulator. Compression seals result in radial compressive stresses within the insulator (with maximum stresses at the interfaces) [40]. Applied tension must first overcome the residual compressive stresses before producing tension within the insulator. Furthermore, the compression can mechanically increase the hermeticity of imperfectly bonded interfaces.

Thermal expansion mismatches between the sealing materials results in the formation of residual stresses. The magnitude of the residual thermal stresses can be estimated by the equation:

$$\sigma_R = CE \int_{T_R}^{T_0} \Delta \alpha dT$$

where E is the elastic modulus, $\Delta\alpha$ is the difference in CTE between the components ($\alpha_{\text{metal}} - \alpha_{\text{insulator}}$), T_0 is the processing temperature (e.g. the glass transition temperature or the brazing temperature), T_R is the service temperature, and C is a geometry and relative thickness-dependent constant [14]. Residual axial compressive stresses and shear stresses are produced within the insulator (maximum at the surface) if the body (exterior) of the component has a higher CTE than the insulator. If the strength of the insulator is exceeded at or near the interface, cracks will form near and parallel to the interface. If the bonding of the interface itself is weak, cracks can propagate along the interface and separate the components. Crack initiation near the interface must particularly be avoided.

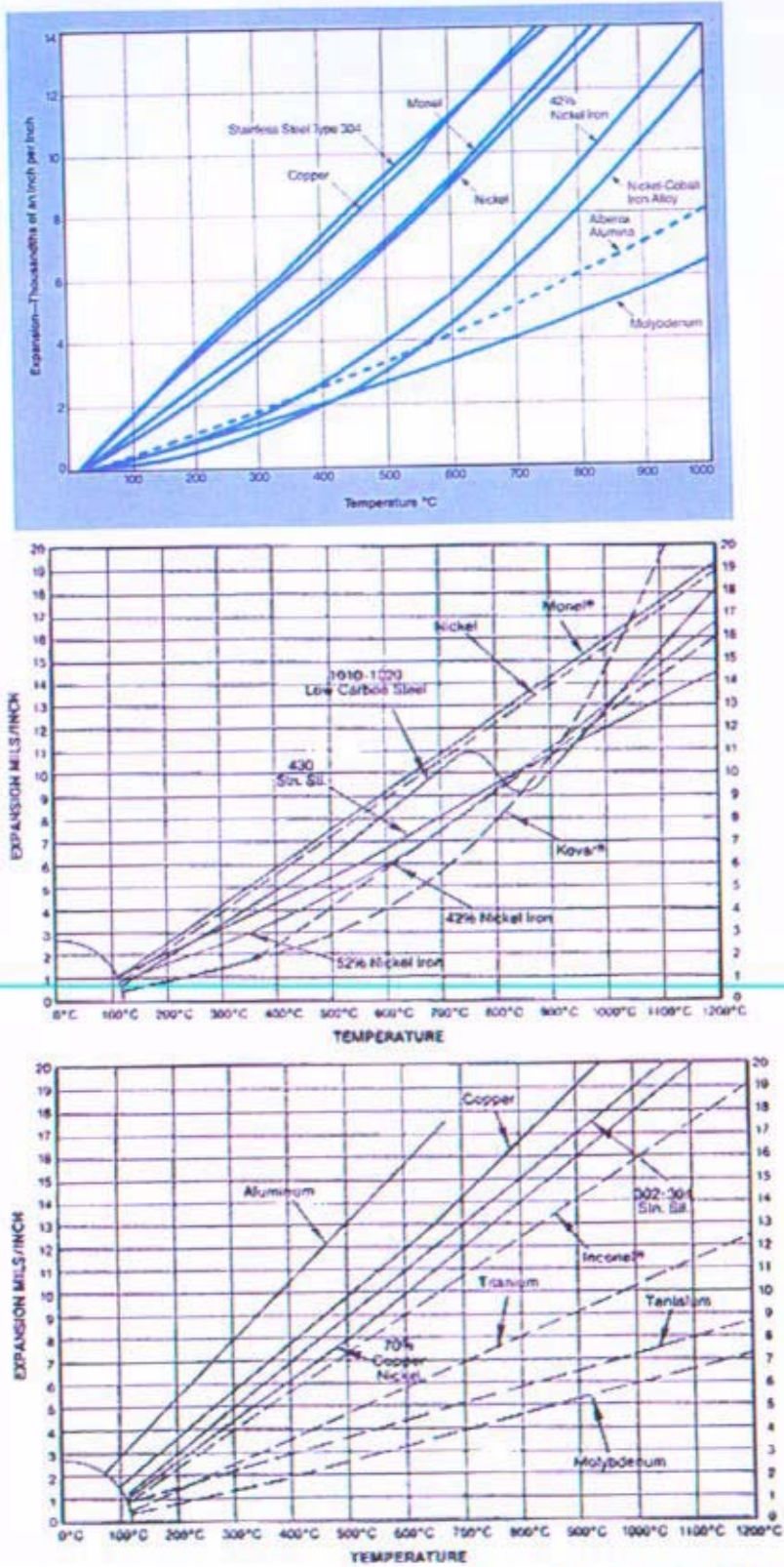


Figure A.1. Approximate thermal expansion of various alloys on heating from room temperature (from References 54 (top) and 5 (middle and bottom)).

Even if cracks form at the interface, fracture theory states that a crack will propagate only if the stress intensity factor at the crack tip (K_I) is greater than the critical stress intensity factor (K_{IC}), or the fracture toughness, of the material ($K_I = K_{IC}$ at failure). The stress intensity (or Griffith) equation is given as:

$$K_I = Y \cdot \sigma \cdot c^{1/2}$$

where σ is the stress, c is the flaw size, and Y is a constant based on crack and loading geometry with value around 1-2 [63]. Typical toughness values for brittle materials range from 0.5 to 1.5 MPa·m^{1/2} for typical silicate glasses to 1 to 20 MPa·m^{1/2} for dense polycrystalline ceramics [40]. While the stress intensity factor at a certain location in the material (i.e. in high tensile or shear stress zones) may exceed the toughness of the material, induced stresses elsewhere in the same material (i.e. residual compressive stress zones) that locally decrease the magnitude of σ may prevent the crack from propagating fully through the material. Therefore, stable cracks can often exist within even brittle materials. However, for the Prometheus application described herein, it is expected that cracks and other similar defects within the material (i.e. near the insulator/metal interface) would create faster diffusion pathways for He (and possibly Xe) gas. Thus, the potential stress fields inside of the feedthrough component and the integrity of the material (especially near the interface) would require thorough characterization.

The CTEs of most materials change significantly with temperature. Therefore, it is imperative to obtain the full trend of CTEs for the materials of interest up to the processing temperature where thermally induced stresses begin to form (i.e. for glasses, the set point or the glass-transition temperature, T_g ; and for ceramics, the braze temperature) in order to determine the thermally induced stresses over the complete range of temperatures involved. A visco-elastic model may be used to more accurately compute the residual stresses for glass/metal seals [40,64].

For many metal/ceramic combinations, the thermal stress incurred while cooling from the processing temperature may yield (plastically deform) the metal. This deformation reduces the residual stresses within the metal. For nominally compressive seals, reheating the yielded metal (assuming that the metal has a higher CTE than the insulator) will then induce tensile stresses in the insulator at a lower temperature than for a non-yielded metal because of the reduction in residual compressive stress.

Thermal shock of the insulator is an important concern for fracture of the feedthrough. The thermal stress generated within a component subjected to a temperature difference, ΔT , is approximated by:

$$\sigma = \frac{\Delta T \alpha E}{1 - \nu}$$

where α is the linear thermal expansion coefficient, E is the elastic modulus, and ν is the Poisson's ratio. Thus, low thermal expansion, high thermal conductivity (reduction of ΔT) materials are desirable to limit the stresses of thermal shock.

The incorporation of multiple wires of diameter D within a single insulating matrix material increases the magnitude of the stress fields. The distance L between wires within the matrix must be sufficiently large to avoid the creation of severe stresses. As a general rule of thumb, L/D must be greater than 0.5; while L/D greater than 1.0 is generally desired [40].

A.3 Surface Wetting

The bonding of dissimilar materials often relies on the formation of a liquid phase at the interface that wets the solid(s) before solidifying to produce a strong hermetic seal. Wetting is driven by a reduction in free energy at the solid surface. The surface energy is defined as the excess free energy at the surface (per unit area) compared to the bulk. The surface energy (SI units of $[J/m^2]$) is always positive in value, because the surface atoms are not fully coordinated. Crystalline metals typically have the highest surface free energies (500 to 2000 ergs/cm²), while ceramics have lower surface energies because of screening of the cations by the anions. Glasses and liquids have lower surface energies (250 to 400 ergs/cm²) due to the slight atomic structural relaxation at the surface. Organic materials generally have the lowest surface energies because of weaker bonding [14,65].

To produce strong bonding, the surfaces must be intimately contacted at the interface. This can be obtained by wetting and spreading of a liquid onto the solid. Wetting is obtained if the free energy of the solid surface, or the solid/vapor surface tension, γ_{sv} , is lowered by contact with the liquid. The balance of surface energies at equilibrium is given by Young's equation as:

$$\gamma_{sv} - \gamma_{sl} = \gamma_{lv} \cos \theta$$

where γ_{sl} is the surface tension of the solid/liquid interface, γ_{lv} is the surface tension of the liquid/vapor interface, and θ is the contact angle between the liquid and solid. For wet surfaces, θ is less than 90°. If the surfaces do not wet, the liquid will not penetrate surface irregularities, and the liquid does not distribute uniformly over the solid. Spreading of the liquid on the surface occurs if $\gamma_{sv} - \gamma_{sl} > \gamma_{lv}$. As spreading extends, the liquid/vapor surface energy causes the resisting force. Wetting can be promoted if the solid dissolves a component of the liquid to change the substrate composition (if the solid has an affinity for the liquid). When the solid substrate dissolves part of the liquid, the free energy of this reaction contributes toward the wetting of the interface and spreading of the liquid. However, spreading does *not* typically occur when the liquid dissolves part of the solid surface (unless the solid surface composition changes) because γ_{sv} is not lowered [65]. Satisfactory wetting for brazing occurs for θ less than about 70° [42].

A.4 Bonding and Interfacial Reactions

Materials can bond at an interface by direct bonding between the materials or by indirect bonding through interfacial phases. The direct bonding of materials, or diffusion bonding, occurs by interdiffusion of atoms across an interface to produce strong bonding between the materials. The interface then contains phases saturated with dissolved atoms, and a balance of bond energies leaves the two phases compatible and at equilibrium [65]. Because of different solubility limits of the phases in contact, the interface moves in the direction necessary to achieve mass balance. As the bonded material cools from the processing temperature, precipitates may form in the phases if the solubility of the phases decreases significantly. Solution bonding is simply diffusion bonding using a molten liquid in contact with a solid surface. Reaction bonding is bonding via a chemical reaction at the interface between two pressed materials (for example, the bonding of Nb to Al₂O₃ with the formation of NbO at the interface).

Generally, metals do not bond strongly to ceramics or glasses *directly* because of the incompatibility of metallic bonding with ionic and covalent structures. Thus, an interfacial phase is often necessary to transition the bonding. This interfacial phase is often an oxide of the metal involved. For instance, bonding of glass to metals usually involves preoxidation of the metal. Molten glass is then applied to the oxidized surface and dissolves a portion of the oxide layer,

providing both the glass/oxide and oxide/metal phase compatibilities. Thicker preoxidized metal layers lead to more gradual composition gradients at the interface [65].

If the preoxidized layer becomes completely dissolved in the glass, then oxidation/reduction (redox) reactions of the underlying metal must occur to form the phase compatibility and to promote adherence. Bonding strength is generally lower if the glass completely dissolves the oxide. Conversely, if the oxide layer is too thick, the remaining oxide layer, its defects (i.e. porosity and cracks), and its bonding strength with the metal largely determine the strength of the seal [14]. For spontaneous redox reactions to occur, the underlying metal must have a higher oxidation potential than a cation in the glass to produce a negative free energy reaction. Redox reactions are often complex, with the formation of secondary phases in addition to the oxide phases. If multiple phases are formed by the reactions, the interface may be tailored chemically to favor one intermediate phase over the others [65]. One theory states that "the most stable interface is one where there is an intermediate layer saturated in a cationic species that is in equilibrium with the parent phases" [17]. Thus, at equilibrium the valence of the cations in the reaction layer are intermediate between the metal and the ceramic or glass.

A.5 Metal Brazing

If it is not feasible to produce strong interfacial bonds at a joint between dissimilar materials, brazing may be used to join the materials. Eutectic metal systems are often used for brazing metals. While diffusion bonding of brazes with the metal substrates occurs readily, the main components in brazing alloys generally neither wet nor react with the ceramics. Therefore, a small but optimized content of reactive metal (e.g. 1-5 wt% titanium or zirconium) is usually added to the brazing alloy to promote reaction with the ceramic and to form a compatible intermediate ceramic phase that promotes wetting and spreading of the brazing alloy along the interface. For example, an intermediate oxide may form at the interface (e.g. Al_2TiO_5 in Al_2O_3 systems with Ti in the braze alloy) along with the dissolution of some of the metal atoms from the ceramic phase, and some of the ceramic itself, into the braze metal (e.g. Al and Al_2O_3 may dissolve into the braze alloy) [16]. Excess reactive metal concentration in the braze alloy can lead to an increase in liquidus temperature and hardening and embrittlement of the filler alloy [17]. Common braze filler metals are based on gold, copper, silver, titanium, lead and tin [41]. Active metal additives include Ti, Zr, Al, Si, Mn, Li, and alloys of these metals.

Important variables pertaining to the brazing process and resulting properties include the following: active metal content of the filler metal, dwell time above the liquidus temperature, heating and cooling rates, pressure, form of braze alloy (e.g. foil or paste), thickness of braze alloy, purity of atmosphere during brazing, and surface roughness of the joined materials [43].

Indirect brazing can also be performed, where the ceramic surface is coated with a secondary material prior to brazing. This secondary material promotes wetting of the surface that would otherwise not be wet by the braze alloy. This technique is also called "metallizing" of the ceramic surface, as described below.

A.6 Indirect Brazing and Metallizing of a Ceramic Surface

Indirect brazing is commonly used for preparing ceramic/metal joints, and is the preparation of a ceramic for brazing by forming a wetting, reactive surface. Painting of metal-containing inks, sputtering a metallic target, or vapor deposition of a metal, with subsequent thermal decomposition, are the primary methods of metallizing ceramic surfaces.

Successful metallization layers must be strongly adhered to both the ceramic and metal surfaces. The metal layer should not be brittle, and it should be of proper thickness for the system. An example of a metallizing system is the molybdenum-manganese process to metallize alumina. A mixture of Mo (~90 at.%) and Mn (~10 at.%) is applied to the ceramic surface. The ceramic is then sintered above 1675 K (2550°F) in hydrogen and nitrogen. The sintering process draws glassy material from the alumina into the Mo powder interstices through a low-viscosity MnO glass. The glassy phase at the interface bonds to the metal and to the ceramic, resulting in a bonded, graded interface. The enhancement of the bond created by metallizing the surface is most likely due to the thicker, graded interfacial zone that lowers the interfacial stresses [65]. The Mo coating can also be plated with a braze-enhancing metal (i.e. nickel or copper) to promote brazing with conventional filler metals. An example of a metallized ceramic is an alumina substrate bonded to a dense, ~25 μm (1 mil) thick Mo layer covered by a 2.5-7.5 μm (0.1-0.3 mil) thick layer of nickel [41].

A.7 Solid State or Diffusion Bonding

Solid state joining of ceramics to metals can be accomplished if there is sufficient interdiffusion of atoms between the ceramic and metal. Solid-state bonding can be produced through diffusion bonding, reaction bonding, pressure bonding and solid-state welding. The driving force for solid state bonding is a reduction in the surface energy between the components. Reactions between the materials can further lower the system energy, increasing the strength of the bond. However, excessive formation of reaction product layers can weaken the joint [43]; for example, by the formation of weak and/or brittle intermetallics. Processing temperatures, pressures, and times are all generally higher for solid-state bonding than for liquid bonding processes.

Interlayers may also be used for solid state bonding. For example, aluminum foil has been used as a solid-state interlayer to bond metals to alumina. Metallization layers can also be used as diffusion bonding interlayers. Mixtures of ceramic and metal powders may be used as interlayers to minimize residual stresses at the interface [16].

Temperatures for solid state joining typically range from about 0.5 to 0.8 of the melting point of the lowest melting component in the system. Applied pressures range from 15 kPa (3 psi) to over 200 MPa (29 ksi), for durations ranging from 1 to 10^4 seconds [42,43]. Higher pressures are required to produce intimate contact between rougher surfaces; therefore smoother ceramic surfaces are desirable for solid state bonding. Generally, one of the components, usually the metal, plastically deforms under the applied load. Deformation of the metal portion of the joint can clean the oxide surface of the metal to promote bonding. Materials processes associated with elevated temperature pressure joining include plastic flow, creep deformation, and diffusion along surfaces and grain boundaries or through the bulk of a grain [43]. Surface cleanliness is a major issue, and the surfaces to be joined must be free of impurities, including hydrocarbons from organic processing agents [42]. Joining is most often performed in vacuum to avoid deleterious reactions.

A.8 Direct Bonding or Fusion Welding

The welding of components by melting the edges of the components or by using melt of a filler of similar materials has been used in the past to produce ceramic/metal and glass/metal seals. There are many shortcomings associated with this method, including the necessity of a close match of melting points and thermal expansion coefficients of the materials to be joined and any created phases; the evaporation or sublimation of components near their melting points; disruptive phase transformations upon cooling; stress fractures due to temperature gradients; and cracking due to increase in ceramic grain size in the weld zone. An electron beam (small spot size, good atmospheric control) has been used in the past to perform fusion welding between alumina insulators and Mo, Nb, W, Ta, and Kovar[®] (Fe-Ni-Co low expansion) alloys [42,66]. Arc welding has been used to join zirconia with Mo, Nb, and Ta as well as graphite with tungsten [42].

CONCURRENCE RECORD SHEET

- DOCUMENT NUMBER: B-MT(AMSI)-44
- THIS DOCUMENT CONTAINS INFORMATION WHICH SHOULD BE CONSIDERED FOR PATENT DISCLOSURES YES NO
- THIS DOCUMENT CONTAINS INFORMATION WHICH MEETS BETTIS WORK CATEGORIES [A,B,C,D or (N/A)] N/A

CONCURRENCE SIGNATURES (Activity must be included) - RESOLVE COMMENTS BEFORE SIGNING

| SIGNATURE/ACTIVITY | DATE | TYPE | DETAILS OF REVIEW REQUESTED (if necessary) |
|-----------------------|-----------------|----------|--|
| <i>R. Messham for</i> | <u>12/20/05</u> | <u>3</u> | |
| M. Postlethwait, KAPL | <u>12/20/05</u> | <u>3</u> | |
| <i>R. Messham for</i> | <u>12/20/05</u> | <u>3</u> | |
| K. C. Loomis, KAPL | <u>12/20/05</u> | <u>3</u> | |
| <i>W. L. Ohlinger</i> | <u>12/20/05</u> | <u>3</u> | |
| W. L. Ohlinger, MT | | | |

TYPE OF REVIEWS (to be determined by author) [See table at end of instructions for definitions.]

1-Peer:Summary 2-Peer:Intermediate 3-Peer:Detail 4-Independent 5-Informal Committee 6-Formal Committee 7-Specialist 8-Interface

NAME TYPED AND SIGNATURE OF NEXT HIGHER MANAGER NOT SIGNING ON LETTER DATE

John E. Hack 11/3/06
J. E. Hack, Manager, Advanced Materials Technology

• CONTRIBUTORS AND IMPACTED PARTIES NOT REQUESTED TO CONCUR AND WHY:

None

DISTRIBUTION

Bettis

NR

KAPL

PNR

M. N. Smith - 02B/GM
S. D. Harkness - 01Q/MT
M. J. Zika - 01C/SE
J. E. Hack - 05R/MT
R. L. Messham - 14B/MT
R. Baranwal - 05R/MT
C. W. Clark, 01C/SE
C. D. Eshelman, 36E/SE
D. Hagerty, 38D/SE
R. C. Jewart, 01C/SE
A. M. Datesman, 14B/MT
A. M. Ruminski, 61F/NEO
C. B. Geller, 33F/RT
R. J. Blasi, 14B/MT

M. Natale, 08I/8024
J. D. Yoxtheimer, 08S/8034
T. H. Beckett, 08B/8012
S. Bell, 08I/8024
D. I. Curtis, 08S/8034
D. E. Dei, 08A/801
T. N. Rodeheaver, 08I/8024
S. J. Rodgers, 08E/8019

S. Simonson, 92
M. Frederick, 92
J. M. Ashcroft, 132
P. F. Baldasaro, 111
C. F. Dempsey, 93
K. C. Loomis, 132
D. F. McCoy, 111
H. Schwartzman, 132
M. J. Wollman, 111
M. Postlethwait, 92
L. S. Donovan, 92
B. C. Campbell, 92
S. J. Belanger, 92
L. E. Kolaya, 92

S. C. Berasi
S. Kraynik
J. Andes
R. J. Argenta
H. A. Cardinali
J. F. Koury
G. White

Bettis (Continued)

J. K. Clobes, 05R/MT
W. L. Ohlinger, 05R/MT

BPMI-P

SNR

S. D. Gazarik
R. F. Hanson

G. M. Millis, 065
D. Clapper, 065
S. Cramer, 065
W. Leahy, 065
H. Miller, 065
D. J. Potts, 065

BPMI-S

F. Barilla

